A REDUCED COMPLEXITY HYBRID PRECODING ARCHITECTURE AND USER GROUPING ALGORITHMS FOR DOWNLINK WIDEBAND MASSIVE MIMO CHANNELS

A THESIS SUBMITTED TO
THE GRADUATE SCHOOL OF NATURAL AND APPLIED SCIENCES
OF
MIDDLE EAST TECHNICAL UNIVERSITY

BY

EMRE KİLCİOĞLU

IN PARTIAL FULFILLMENT OF THE REQUIREMENTS
FOR
THE DEGREE OF MASTER OF SCIENCE
IN
ELECTRICAL AND ELECTRONICS ENGINEERING

SEPTEMBER 2019

Approval of the thesis:

A REDUCED COMPLEXITY HYBRID PRECODING ARCHITECTURE AND USER GROUPING ALGORITHMS FOR DOWNLINK WIDEBAND MASSIVE MIMO CHANNELS

submitted by **EMRE KİLCİOĞLU** in partial fulfillment of the requirements for the degree of **Master of Science in Electrical and Electronics Engineering Department, Middle East Technical University** by,

Prof. Dr. Halil Kalıpçılar
Dean, Graduate School of **Natural and Applied Sciences** _____

Prof. Dr. İlkay Ulusoy
Head of Department, **Electrical and Electronics Engineering** _____

Assist. Prof. Dr. Gökhan Muzaffer Güvensen
Supervisor, **Electrical and Electronics Engineering, METU** _____

Examining Committee Members:

Prof. Dr. Ali Özgür Yılmaz
Electrical and Electronics Engineering, METU _____

Assist. Prof. Dr. Gökhan Muzaffer Güvensen
Electrical and Electronics Engineering, METU _____

Prof. Dr. Engin Tuncer
Electrical and Electronics Engineering, METU _____

Prof. Dr. Emre Aktaş
Electrical and Electronics Engineering, Hacettepe University _____

Assoc. Prof. Dr. Melda Yüksel Turgut
Electrical and Electronics Engineering, TOBB University _____

Date:

I hereby declare that all information in this document has been obtained and presented in accordance with academic rules and ethical conduct. I also declare that, as required by these rules and conduct, I have fully cited and referenced all material and results that are not original to this work.

Name, Surname: Emre Kilcioğlu

Signature :

ABSTRACT

A REDUCED COMPLEXITY HYBRID PRECODING ARCHITECTURE AND USER GROUPING ALGORITHMS FOR DOWNLINK WIDEBAND MASSIVE MIMO CHANNELS

Kilcioğlu, Emre
M.S., Department of Electrical and Electronics Engineering
Supervisor: Assist. Prof. Dr. Gökhan Muzaffer Güvensen

September 2019, 92 pages

In this thesis, an efficient hybrid precoding architecture is proposed for single-carrier (SC) downlink wideband spatially correlated massive multiple-input multiple-output (MIMO) channels. The design of two-stage beamformers is realized by using a virtual sectorization via second-order channel statistics based user grouping. The novel feature of the proposed architecture is that the effect of both inter-group-interference (due to non-orthogonality of virtual angular sectors) and the inter-symbol-interference (due to SC wideband transmission) are taken into account. While designing the analog beamformer, we examine the dimension reduction problem and proper subspace (beamspace) construction (by exploiting the joint angle-delay sparsity map and power profile of the multi-user channel) based on which a highly efficient spatio-temporal digital precoding is proposed. Before the beamforming stage, the user terminals are distributed into multiple groups by using their second order statistics via a user grouping algorithm named as merge and split based algorithm with K-means initialization and our own performance metric. This algorithm finds an optimal user grouping distribution to maximize the performance of the hybrid precoding structure. If

the proposed joint angle-delay generalized eigen beamformer (JAD-GEB) type analog beamformer, reduced complexity spatio-temporal channel matched filter-spatially regularized zero forcing (CMF-SZF) type digital precoder and merge and split based user grouping algorithm with K-means initialization and our own performance metric are utilized together for the hybrid structure, the performance results reach very close to those of the fully digital CMF type precoding by using less number of RF chains.

Keywords: Massive MIMO, millimeter wave, hybrid, beamforming, user grouping, downlink, achievable information rate

ÖZ

DOWNLİNK GENİŞ BANT MASSİVE MIMO KANALLARI İÇİN KARMAŞIKLIĞI AZALTILMIŞ HİBRİT ÖN KODLAMA MİMARİSİ VE KULLANICI GRUPLANDIRMA ALGORİTMALARI

Kilcioğlu, Emre
Yüksek Lisans, Elektrik ve Elektronik Mühendisliği Bölümü
Tez Yöneticisi: Dr. Öğr. Üyesi. Gökhan Muzaffer Güvensen

Eylül 2019 , 92 sayfa

Bu tezde, uzamsal olarak korelasyonlu Massive MIMO kanalları için tek taşıyıcı downlink geniş bant için etkili bir hibrit ön kodlama mimarisi önerilmiştir. İki aşamalı ışın biçimlendiricilerin tasarımı, ikinci dereceden kanal istatistiklerine dayalı kullanıcı gruplandırması yoluyla sanal sektörlendirme kullanılarak gerçekleştirilir. Önerilen mimarinin literatüre katkısı, hem gruplar arası girişimin (sanal açısal sektörlerin ortogonal olmasından dolayı) hem de semboller arası girişimin (tek taşıyıcı geniş-bant iletimi nedeniyle) etkisinin dikkate alınmasıdır. Analog ışın biçimlendiriciyi tasarlarken, boyut azaltma problemi ve yüksek verimli bir uzaysal-zamansal dijital ön kodlamanın önerildiği temel alt uzay (ışın alanı) yapısı (ortak açılı gecikme sparsity haritasını ve çok kullanıcılı kanalın güç profilini kullanarak) incelenmektedir. Işın biçimlendirme aşamasından önce, kullanıcı terminalleri, K-means ilklendirmesi ve performans metriği ile birlikte birleştirme ve bölme tabanlı algoritma olarak adlandırılan bir kullanıcı gruplandırma algoritması yoluyla kullanıcıların ikinci dereceden istatistiklerini kullanarak çoklu gruplara dağıtılır. Bu algoritma hibrit ön kodlama yapısının

performansını en üst düzeye çıkarmak için optimum bir kullanıcı gruplandırma dağılımı bulur. Önerilen JAD-GEB analog ışın biçimlendirmesi, CMF-SZF türü dijital ön kodlama ve K-means ilklendirmesi ve AIR metriği ile birlikte birleştirme ve bölme tabanlı kullanıcı gruplandırma algoritması beraber kullanıldığında performans sonuçları tamamen dijital bir CMF tipte bir ön kodlama kullanılarak oluşturulan performans sonuçlarına çok yakın çıkmaktadır.

Anahtar Kelimeler: Massive MIMO, milimetre dalga, hibrit, hüzme, kullanıcı gruplama, ulaşılabilir bilgi oranı

To my lovely wife and my family

ACKNOWLEDGMENTS

I would like to express my sincere gratitude to my advisor Assist. Prof. Dr. Gökhan Güvensen, in this thesis for guidance, patience, suggestions, encouragement, hard-working and insight. These were extremely precious for me throughout the research. Besides these, weekly meetings with him contribute a lot to improve myself and develop such a research. Without the recommendations that he gave to me, I would not proceed with this research. It was a great pleasure for me to work with him.

I would like to thank ASELSAN Inc. for which I have been working throughout my master of science study to let me attend the lectures freely at working hours. I also appreciate my managers at ASELSAN Inc. for their helps, understanding and patience during my research. I am also grateful to my colleagues at ASELSAN Inc. to help me gain some experience for my career and my research.

I am truly thankful to The Scientific and Technological Research Council of Turkey (TÜBİTAK) for its financial support during my master of science research study.

I am indebted to my parents, Suat Kilcioğlu and Zübeyde Kilcioğlu, and my sister, Elif Kilcioğlu, for their endless support during all my education including master of science study. I truly owe so much to them.

Last but not the least; I give my best gratitudes to my dear wife, Şeyma, for her patience, understanding and endless support during all my life including the preparation of this thesis. She gives me strength invariably and she has always been a pushing force for me to complete my research.

TABLE OF CONTENTS

LIST OF TABLES

TABLES

LIST OF FIGURES

FIGURES

LIST OF ABBREVIATIONS

AIR	Achievable Information Rate
AoA	Angle of Arrival
AO-EB	Angle Only Eigen Beamformer
AO-GEB	Angle Only Generalized Eigen Beamformer
AWGN	Additive White Gaussian Noise
BS	Base Station
CCM	Channel Covariance Matrix
CMF	Channel Matched Filter
CSI	Channel State Information
DFT	Discrete Fourier Transform
HDA	Hybrid Digital/Analog
ISI	Inter-Symbol Interference
JAD-EB	Joint Angle Delay Eigen Beamformer
JAD-GEB	Joint Angle Delay Generalized Eigen Beamformer
JSDM	Joint Spatial Division and Multiplexing
MIMO	Multiple-Input and Multiple-Output
MPC	Multi-Path Component
NOMA	Non Orthogonal Multiple Access
PADP	Power Angle-Delay Profile
RF	Radio Frequency
SC	Single Carrier
SINR	Signal to Interference and Noise Ratio
SNR	Signal to Noise Ratio
SZF	Spatial Zero Forcing

TDD	Time Division Duplex
TDMA	Time Division Multiple Access
TX	Transmit
ULA	Uniform Linear Array
UT	User Terminal

NOMENCLATURE

$\beta^{(g_k)}$ Desired signal gain

$\mathbf{\Theta}_l^{(g',g)}$ Covariance matrix of $\mathbf{R}_l^{(g',g)}$

$\Delta\theta_l^{(k)}$ Angular spread of the l^{th} multi-path component of the k^{th} user terminal

$\gamma^{(k)}$ Squared Channel gain of the k^{th} user terminal at the base station

Λ Optimal intra-group RF chain distribution

$\lambda_{l,n}^{(g)}$ n^{th} generalized eigenvalue of the analog beamforming matrix $\mathbf{S}^{(g)}$

$\mathbf{\Phi}^{(g',g)}$ Matrix containing all effective reduced dimensional channels as row matrices

$\boldsymbol{\phi}_k^{(g',g)}$ k^{th} column vector of $\mathbf{\Phi}^{(g',g)}$

$\rho_l^{(k)}(\theta)$ Power angle-delay profile (PADP) of the l^{th} multi-path component of the k^{th} user terminal

$\boldsymbol{z}$ Complex, zero mean, unit variance and normally distributed random $N \times 1$ vector

$\mathbf{a}(\theta)$ Unit norm steering vector at the angle θ

$\mathbf{B}$ Analog beamforming matrix

$\mathbf{d}_n$ $K \times 1$ desired signal vector that is wanted to be transmitted to all groups at time index n

$\mathbf{d}_n^{(g)}$ $K_g \times 1$ desired signal vector for only group g user terminals at time index n

$\mathbf{E}_{K,k}$ $K \times K$ matrix whose elements are all zero except the k^{th} diagonal entry

$\mathbf{F}()$ Digital precoder matrix operator

$\mathbf{H}_l$ General statistically sparse channel matrix before user grouping

$\mathbf{H}_l^{(g)}$ General statistically sparse channel matrix for group g user terminals after user grouping

$\mathbf{h}_l^{(g_k)}$ $N \times 1$ multi-path user channel vector for the l^{th} multi-path component (MPC) of k^{th} user terminal in group g after user grouping

$\mathbf{h}_l^{(k)}$ $N \times 1$ multi-path user channel vector for the l^{th} multi-path component (MPC) of k^{th} user terminal before user grouping

$\mathbf{H}_{eff,l}^{(g',g)}$ Effective reduced dimensional channel for the l^{th} multi-path components

$\mathbf{I}_k$ Identity matrix with dimension $k \times k$

$\mathbf{n}_n$ Additive white Gaussian noise (AWGN) vector at time index n

$\mathbf{Q}_l^{(g)}$ Kronecker product of $\mathbf{T}_l$ and $\mathbf{I}_{D_g}$

$\mathbf{R}_l^{(g)}$ Group Channel covariance matrix for the l^{th} multi-path component in group g

$\mathbf{R}_l^{(g_k)}$ Channel covariance matrix for the l^{th} multi-path component of the k^{th} user terminal in group g after user grouping

$\mathbf{R}_l^{(k)}$ Channel covariance matrix for the l^{th} multi-path component of the k^{th} user terminal before user grouping

$\mathbf{R_F}$ Covariance matrix of the digital precoder matrix operator

$\mathbf{R}_{\mathbf{H}_{eff,l}^{(g,g)}}$ Covariance matrix of the effective reduced dimensional channel for the l^{th} multi-path components

$\mathbf{R_y}$ Covariance Matrix of the received signal at the base station for uplink training mode

$\mathbf{R}_{sum}^{(g)}$ Sum of all group channel covariance matrices

$\mathbf{S}^{(g)}$ $N \times D_g$ analog beamforming matrix that reduces the dimension of MIMO channel for group g user terminals

$\mathbf{S}^{(g)}(l)$ Column matrix of the analog beamforming matrix for the l^{th} multi-path component of the group g user terminals

$\mathbf{T}_l$ $L \times L$ matrix where $(m,n)^{th}$ entry is δ_{m-n+l}

$\mathbf{W}_l^{(g)}$ Digital precoding filter that can be changed according to the digital precoder type of the system

$\mathbf{x}_n$ Precoded signal vector at time index n

$\mathbf{y}_n$ Received signal at the base station for uplink training mode

$\mathbf{y}_n^{(g)}$ Received signal vector for all group g user terminals at time index n

$\theta_{l,center}^{(k)}$ Angle of arrival center of the l^{th} multi-path component of the k^{th} user terminal

$\theta_{l,max}^{(k)}$ Maximum Value of the azimuth interval of the l^{th} multi-path component of the k^{th} user terminal

$\theta_{l,min}^{(k)}$ Minimum Value of the azimuth interval of the l^{th} multi-path component of the k^{th} user terminal

Υ User grouping set

$\xi_n^{(g_k)}$ Interference signal gain

$AIR^{(g)}$ Achievable information rate value for group g

AIR_{TOTAL} Total achievable information rate of whole channel

$c^{(g)}$ Power scaling factor to set the downlink channel power scale for each group algorithmically

D Number of RF chains in the system

D_g Number of RF chains allocated for group g user terminals

$d_l^{(g)}$ Number of RF chains allocated for the l^{th} multi-path component of the group g user terminals

$d_n^{(g_k)}$ k^{th} element of the desired signal for the k^{th} user terminal of group g

$e_k^{(g)}$ $K_g \times 1$ vector whose elements are all zero except the k^{th} entry

E_s Total transmit power given to all system

$E_s^{(g)}$ Transmit power for group g user terminals

G Number of groups in the system

K Number of single-antenna user terminals

K_g Number of user terminals in group g

L Total multi-path component number in the system

L_g Number of active multi-path component in group g

N Number of antennas on the base station

N_0 Noise power

$r_n^{(g_k)}$ Received signal by the k^{th} user terminal in group g at time index n

SNR_{TX} Transmit SNR

SNR_{uplink} Uplink SNR

CHAPTER 1

INTRODUCTION

1.1 Motivation

Massive multiple-input multiple-output (MIMO) technology is thought as a possible key technology for the next generation cellular systems like 5G thanks to having a large number of antenna elements at the base station (BS) to serve less number of user terminals (UTs) [1], [2]. Massive MIMO is particularly promising with large gains in both spectral and energy efficiency for outdoor mobile cellular systems that operate at millimeter-wave (mm-wave) frequency bands where very large antenna arrays can be packaged into small forms and have extremely wide bandwidths [3], [4]. Therefore, Massive MIMO technology at mm-wave bands form an important part of future communication systems like 5G that are expected to support approximately 1000 times faster data rates than the current standards [1].

For the precoder, obtaining channel state information (CSI) instantaneously is substantial in Massive MIMO transmission [5]. However, the instantaneous CSI results in the pilot overhead problem [6]. For this purpose, it would be better if the slowly varying channel parameters like long term parameters are taken into account as CSI for the precoder.

For this type of precoder, a fully analog beamforming is not possible because it only supports single stream transmission [7], [8]. In addition, the inherent constraints of cost and energy make it impractical build a fully digital precoder with a complete radio frequency (RF) chain for each antenna element. The two-stage-beamforming structure under the name of Joint Spatial Division and Multiplexing (JSDM) [11], [12], naturally fitting the hybrid digital to analog (HDA) structure, was proposed to re-

duce the usage of RF chain components by reducing the dimension of Massive MIMO channel effectively, and to enable Massive MIMO gains and simplified system operations [13], [14]. Although JSDM was originally proposed as an effective reduced dimensional two-stage downlink precoding for multi-user Massive MIMO systems in frequency division duplex mode, two-stage beamforming can be implemented to the downlink and uplink sides in time division duplex (TDD) mode. The main process before the precoder and beamformer part is the user-grouping, that is, the user terminals are distributed to multiple groups that have approximately the same channel covariance eigenspaces via a novel design of a user grouping algorithm before the precoding operations. With this way, Massive MIMO analog beamformer stage of the proposed precoder at BS easily creates the beams for each group and maximizes intra-group signals by suppressing the inter-group interference and it also reduces the channel dimension by forming a new effective reduced dimensional channel. The MIMO analog beamformer uses the long-term parameters (second order channel statistics), it does not utilize any instantaneous CSI. This is the major reason of the complexity and dimension reduction. JSDM design allows to use HDA beamforming structures, which use a combination of analog beamformers in the RF domain together with a reduced number of RF chains [15], [16], [17]. This hybrid structure is proposed as an alternative for Massive MIMO systems in mm-wave systems because it uses less number of RF chains compared to the fully digital precoder types. This makes the system more power efficient and less complex. In this hybrid architecture, the creation of the beams according to the statistical slowly varying parameters obtained from CSI is operated in the analog RF domain while MIMO precoding and combining stage can be implemented with a standard baseband precoder. The analog beamformer stage of the hybrid structure is considered for frequency selective Massive MIMO channels by using single-carrier (SC) transmission. Contrary to OFDM, SC transmission is preferred so that inter-symbol interference (ISI) is mitigated via the proposed analog beamformer that makes the eigenspaces of each multi-path component (MPC) nearly orthogonal in the spatial domain. Thus, equalization is not necessary in temporal domain for SC transmission. Channel estimation is crucial for the analog beamformer. For this reason, it is assumed that CSI and second order statistics (channel covariance matrices) of each UT are perfectly obtained without no error for this research to observe how well the hybrid precoding structure works when a perfect CSI is taken

as an input. A statistical analog beamformer, namely, joint angle-delay generalized eigen beamformer (JAD-GEB) is proposed. The novel feature of this is that the effect of both inter-group interference (due to non-orthogonality of virtual angular sectors) and inter-symbol interference (due to single carrier wideband transmission) are taken into account. It suppresses the inter-group interference to very low levels. For the digital precoding stage, a highly efficient spatio-temporal channel matched filter (CMF) type digital precoder, namely, channel matched filter-spatially regularized zero forcing (CMF-SZF) type digital precoder is proposed. It eliminates ISI completely, if it is utilized with the proposed analog beamformer, JAD-GEB. It also mitigates intra-group interference.

The wideband Massive MIMO channel at mm-wave frequencies can be said as sparse both in angle and delay domains [18]-[21]. The base station observes the MPCs of each UT channel under an angular range, i.e., angle-of-arrival (AoA) values, and therefore, MPCs are observed in clusters in angle-delay plane [22], [23]. This sparsity allows virtual sectorization (user-grouping) of UTs in angle-delay domain, and efficient pre-processing to reduce dimensionality in analog domain [24].

1.2 Contribution of the Thesis

The main aim of this research is to design a novel hybrid precoding scheme for SC transmission together with a user grouping algorithm that gives an optimal user grouping to obtain the best performance of the hybrid structure. There are several contributions of the thesis on literature.

The first contribution is the proposed analog beamformer that is called as the joint angle-delay generalized eigen beamformer (JAD-GEB). The novel feature of this is that inter-group interference and ISI are all taken into account. It is constructed by using the strongest generalized eigenbeams of intra-group and inter-group signal covariance matrices. These eigenbeams are combined to construct analog beamformer while guaranteeing the orthogonality of effective MPCs in reduced dimensional subspace. The proposed statistical analog beamformer outperforms nearly optimal by comparing it with a nearly full digital structure.

Secondly, a highly efficient spatio-temporal channel matched filter (CMF) type digital processing, namely Channel Matched Filter-Spatial Zero Forcing (CMF-SZF) type precoder, that eliminates ISI completely and mitigates intra-group interference, is proposed for the digital precoder stage of the structure. This reduces the complexity in digital domain, considerably, by using a new reduced dimensional effective channel. This channel is created by using the intantaneous channel and analog beamformer matrices.

To create each beam without having any inter-user interference, a merge and split based user grouping algorithm with K-means initialization is designed with our novel performance metric. Given a user grouping set, the performance metric is calculated by using the proposed analog beamformer and CMF type digital precoding with TDMA type multiplexing for intra-group UTs. The user grouping algorithm finds the optimum user grouping distribution that maximizes the performance of the system before analog beamforming.

Different plots are shown for different perspectives of the effect of transmit powers or user grouping algorithm on the performance of the hybrid precoder architecture. For the transmit power plots, a genie-aided matched filter bound (when inter-group interference and ISI are completely removed after fully digital CMF) is made use of to compare the analog beamformer performances with an ideal fully theoretical bound.

1.3 Outline of the Thesis

Chapter 2 represents a received signal system model about the topic. The channel that we worked on and the effective channel that is designed to obtain a reduced complexity channel are mentioned in this chapter. Also, long term parameters such as the channel covariance matrices are defined and expressed the calculation method of these matrices when the precoder in BS has CSI about UTs in the system.

In Chapter 3, the proposed hybrid beamforming precoder architecture for wideband downlink Massive MIMO channels is mentioned. The hybrid structure has two stages, the analog beamformer and the digital precoder. Different types of analog beamformers and digital precoders are investigated to find the optimal ones. For the analog

beamformer, five types of analog beamformers are investigated and compared into the simulation results section of the thesis. These analog beamformers are named as conventional DFT beamformer, angle only eigen beamformer (AO-EB), joint angle-delay eigen beamformer (JAD-EB), angle only generalized eigen beamformer (AO-GEB) and the proposed joint angle-delay generalized eigen beamformer (JAD-GEB). As the digital precoder, two options are preferred for this study as CMF type precoder and a modified version of CMF type precoder, namely Channel Matched Filter-Spatial Zero Forcing (CMF-SZF) type precoder. In the simulation results of the study, CMF type precoder is divided into two parts according to the usage of TDMA in it. Besides the analog beamformer and digital precoder stages, RF chain distribution to the groups and to the MPCs within the group is adverted in Chapter 3.

In Chapter 4, performance parameter is stated in order to test the performance of different designs of the hybrid precoder in terms of achievable information rate (AIR) which is a kind of user averaged spectral efficiency definition. The analytical solutions to AIR are obtained for CMF type digital precoder part by part with the mathematical operations.

Besides the hybrid structure of this research, the user grouping is also very crucial in order to obtain the best performance from the precoder. For this purpose, an optimal user grouping algorithm is designed in Chapter 5. The optimum user grouping algorithm is found as merge and split based user grouping algorithm with K-means initialization together with novel designed performance metric.

In Chapter 6, the simulation results from different perspectives to AIR changes and the discussions about the design are spoked of. The results show that the nearly optimal hybrid structure is designed with joint angle-delay generalized eigenbeamformer (JAD-GEB) and Channel Matched Filter-Spatial Zero Forcing (CMF-SZF) type precoder together with the merge and split based user grouping algorithm with K-Means initialization and our own performance metric.

Finally, conclusion is provided in Chapter 7 with a summary and the contribution of the research. Future studies are also mentioned in this chapter.

CHAPTER 2

SYSTEM MODEL

2.1 Introduction

The studied system is based on Massive MIMO transmission in mm-wave bands and TDD mode employing SC transmission. At the transmitter side, the base station has N number of antenna elements. On the other hand, at the receiver side, there are K number of single-antenna user terminals. All UTs are grouped into G different groups through a user grouping algorithm according to their second order channel statistics (channel covariance matrices). The algorithm partitions the user population supported by BS into multiple groups each with approximately the same channel covariance eigenspaces [11], [13]. After taking the CSI in uplink training mode, the channel covariance matrices (CCMs) of each user terminal are calculated before the UTs are distributed into the groups. With the CCMs of all user terminals, the algorithm finds the optimal user grouping set that maximizes the performance of the precoder. As an output, it gives the CCMs of each group (not the user terminals) to the analog beamformer part and the analog beamformer creates the beams of each group according to these grouping set. The details of the user grouping algorithm can be found in Chapter 5. The number of user terminals in group g after user grouping is K_g. All user terminals have statistically independent channels. After the user terminals pass through the user grouping algorithm and analog beamformer creates the beams of each group, an effective reduced dimensional channel is defined for each group by using the instantaneous channel and the analog beamformer matrices of each group and it has all channel information of the user terminals. It is the projection of the instantaneous channel on the analog beamforming matrices.

Channel estimation for each UT is carried out at the BS by training sequences during uplink transmission and it is assumed in this thesis that CSI for each user terminal is known perfectly. Analog beamformer utilizes long term parameters for beam creation.

Throughout this chapter, the following notations are used. While the bold lowercase letters denote a vector, the bold uppercase letters denote a matrix. $(\cdot)^H$ is the Hermitian transpose of a vector or a matrix. An identity matrix with dimension $k \times k$ is shown as $\mathbf{I}_k$. The trace operator is denoted as $\mathrm{Tr}\{\cdot\}$. The expected value operator for a vector or a matrix is represented as $\mathbb{E}\{\cdot\}$ and $\mathrm{bdiag}\{\cdot\}$ symbolizes the block diagonal matrix of the given matrix. The absolute value of a scalar is shown as $|\cdot|$, while the norm of a matrix is demonstrated as $\|\cdot\|$.

2.2 Signal Model for Wideband Downlink Massive MIMO Systems

Let the received signal vector $\mathbf{y}_n^{(g)}$ for all group g user terminals at time index n is

$$\mathbf{y}_n^{(g)} = \sum_{l=0}^{L-1} [\mathbf{H}_l^{(g)}]^H \mathbf{x}_{n-l} + \mathbf{n}_n \tag{2.1}$$

where L is the total MPC number in the system, $\mathbf{H}_l^{(g)}$ is the general statistically sparse channel matrix for group g user terminals, $\mathbf{x}_n$ corresponds to the precoded signal vector or the hybrid structure vector at time index n and $\mathbf{n}_n$ is the additive white Gaussian noise (AWGN) vector at time index n. The hybrid structure of this precoder is composed of both analog and digital parts and this structure is represented in the precoded signal vector $\mathbf{x}_n$.

2.3 Statistical Models for Sparse Massive MIMO Channel

Massive MIMO channel acquisition is obtained at the BS in TDD mode. Given the channel covariance matrices of all user terminals, the instantaneous channel is estimated by uplink training sequences. As it is said in Section 2.1, it is assumed that the CSI for each user terminal is known perfectly with no error at the BS. Therefore, the

instantaneous channel is estimated correctly given perfect CSI. The channel of each user terminal and its multi-path components is defined as $\mathbf{h}_l^{(k)}$ before user grouping and each $\mathbf{h}_l^{(k)}$ is calculated independently from each other by using the channel covariance matrix $\mathbf{R}_l^{(k)}$ before user grouping. After they are calculated, they constitute the column vectors of the general statistically sparse channel matrix before user grouping $\mathbf{H}_l$ that is expressed as

$$\mathbf{H}_l = \left[\begin{array}{cccc} \mathbf{h}_l^{(1)} & \mathbf{h}_l^{(2)} & \dots & \mathbf{h}_l^{(K)} \end{array} \right]_{N \times K} \tag{2.2}$$

where $\mathbf{h}_l^{(k)}$ is $N \times 1$ multi-path user channel vector for the l^{th} multi-path component (MPC) of k^{th} user terminal before user grouping is made.

With the instantaneous channel, some long-term channel parameters such as channel covariance matrix (CCM) $\mathbf{R}_l^{(k)}$ of each user terminal for the l^{th} multi-path component of the k^{th} user terminal are also utilized by the user grouping algorithm and the analog beamformer and these parameters can be obtained by using the joint angle-delay power profile of the channel with the angle of arrival (AoA) information and the angular spreads of each multi-path component (MPC) of the user terminals. The channel covariance matrix $\mathbf{R}_l^{(k)}$ can be characterized as

$$\mathbb{E}\left\{ \mathbf{h}_l^{(k)} \left(\mathbf{h}_{l'}^{(k')} \right)^H \right\} = \mathbf{R}_l^{(k)} \delta_{k-k'} \delta_{l-l'} \tag{2.3}$$

where inversely, the multi-path user channel vector $\mathbf{h}_l^{(k)}$ is defined as

$$\mathbf{h}_l^{(k)} = \sqrt{\frac{1}{2}} \sqrt{\mathbf{R}_l^{(k)}} \ \boldsymbol{z} \tag{2.4}$$

where $\boldsymbol{z}$ is a complex, zero mean, unit variance and normally distributed random $N \times 1$ vector. Then, $\mathbf{h}_l^{(k)} \sim CN(0, \mathbf{R}_l^{(k)})$. Here, we assume spatially correlated, Rayleigh distributed vector channels. This is a common assumption for mm-wave Massive MIMO channels [31], [32]. The channel covariance matrix $\mathbf{R}_l^{(k)}$ is calculated for each user terminal with the help of phased array systems by using the unit norm steering

vector $\mathbf{a}(\theta)$ as follows:

$$\mathbf{R}_l^{(k)} = \int_{\theta_{l,min}^{(k)}}^{\theta_{l,max}^{(k)}} \rho_l^{(k)}(\theta)\, \mathbf{a}(\theta)\, (\mathbf{a}(\theta))^H\, d\theta \tag{2.5}$$

where $\rho_l^{(k)}(\theta)$ is the power angle-delay profile (PADP) of the l^{th} multi-path component of the k^{th} user terminal. It also contains the near-far effects of the user terminals. For all θ, some of $\rho_l^{(k)}(\theta)$ parameter might be zero for some multi-path component index l because of working on a sparse channel. By this way, if the k^{th} user terminal does not have any multi-path component on multi-path component l, the channel covariance matrix $\mathbf{R}_l^{(k)}$ of the k^{th} user terminal for l^{th} multi-path becomes a zero matrix. $\theta_{l,min}^{(k)}$ and $\theta_{l,max}^{(k)}$ are the azimuth interval boundaries of the l^{th} multi-path component of the k^{th} user terminal. That is,

$$\begin{aligned} \theta_{l,min}^{(k)} &= \theta_{l,center}^{(k)} - \frac{\Delta\theta_l^{(k)}}{2} \\ \theta_{l,max}^{(k)} &= \theta_{l,center}^{(k)} + \frac{\Delta\theta_l^{(k)}}{2} \end{aligned} \tag{2.6}$$

where the angle of arrival center and the angular spread of the l^{th} multi-path component of the k^{th} user terminal are named as $\theta_{l,center}^{(k)}$ and $\Delta\theta_l^{(k)}$, respectively. $\mathbf{a}(\theta)$ is the unit norm steering vector for the azimuth angle θ and the steering vector $\mathbf{a}(\theta)$ is created by using uniform linear array (ULA) structure with N number of elements as in Eqn.(2.7).

$$\mathbf{a}(\theta) = \begin{bmatrix} 1 & e^{-j\pi\cos(\theta)} & e^{-j2\pi\cos(\theta)} & \dots & e^{-j(N-1)\pi\cos(\theta)} \end{bmatrix}^H \tag{2.7}$$

In order to take the near far effect of the user terminals to the base station into account, a near far effect parameter should be defined in $\mathbf{R}_l^{(k)}$. For this purpose, the channel covariance matrices of the user terminals are generated by obeying the following

equation:

$$\sum_{l=0}^{L-1} \mathrm{Tr}\left\{\mathbf{R}_l^{(k)}\right\} = \gamma^{(k)} \tag{2.8}$$

where L is the number of multi-path components in the system and $\sqrt{\gamma^{(k)}}$ is the channel gain of the k^{th} user terminal at BS and it comes from the near far effect of the user terminals.

After user terminals are distributed into the groups through the user grouping algorithm, the channel covariance matrix and the multi-path user channel vector of the l^{th} MPC of k^{th} user terminal in group g are shown as $\mathbf{R}_l^{(g_k)}$ and $\mathbf{h}_l^{(g_k)}$, respectively. Here, $\{g_k\}_{k=1}^{K_g}$ are user terminal indices. By this way, the general statistically sparse channel matrix for group g user terminals after user grouping is demonstrated as

$$\mathbf{H}_l^{(g)} = \left[\begin{array}{cccc} \mathbf{h}_l^{(g_1)} & \mathbf{h}_l^{(g_2)} & \dots & \mathbf{h}_l^{(g_{K_g})} \end{array} \right]_{N \times K_g} \tag{2.9}$$

User grouping algorithms are discussed in Chapter 5.

2.4 Hybrid Beamforming based Downlink Massive MIMO Systems

In mm-wave communication systems, lots of antennas with large arrays should be utilized in order to obtain an enough power [26]. For this purpose, it is unpractical to implement a fully digital precoder at the base station since it would require a lot of RF chains which make the system consume more power and they also make the system complex. If a fully analog precoder is used, the system only supports single stream MIMO transmission [7]. In order to overcome the power consumption and the complexity problems for fully digital solution and the problem that is not to serve in a multi stream MIMO systems for fully analog solution, a more power efficient and multi user supported hybrid transceiver structure is proposed. In this structure, MIMO processing is splitted between digital and analog parts. By this way, the precoder is able to support in a multi stream MIMO systems thanks to the digital part and less RF chain components can be used by creating a new efficient channel do-

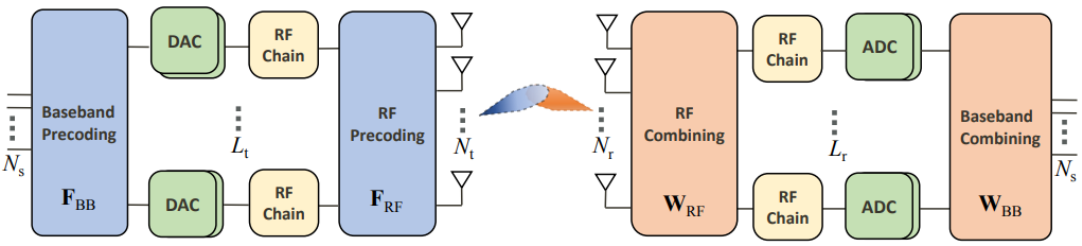

Figure 2.1: Classical Hybrid Beamforming Architecture [30]

main thanks to the analog part of the beamformer. This structure is called the hybrid beamforming structure. A classical hybrid beamforming architecture can be seen in Figure 2.1. In this figure, the number of RF chains L_t and L_r at transmitter and receiver sides is much lower than the number of antennas N_t and N_r at the transmitter and receiver sides, respectively. That is, $L_t << N_t$ and $L_r << N_r$. The proposed hybrid architecture is explained in the next chapter.

CHAPTER 3

A NOVEL HYBRID BEAMFORMING ARCHITECTURE FOR WIDEBAND DOWNLINK MASSIVE MIMO SYSTEM

3.1 Proposed Hybrid Architecture for Single Carrier Transmission

Throughout the thesis, single-carrier transmission is preferred to be the optimal transmission for Massive MIMO channels. The optimality of using single carrier transmission in Massive MIMO channels is justified in [33]. Here, we adopt single-carrier based transmission for hybrid beamforming based Massive MIMO systems and study how to design hybrid architecture for single-carrier based two-stage beamforming where Joint Spatial Division Multiplexing (JSDM) framework is utilized. In JSDM, a statistical user grouping based pre-beamformer is proposed in order to reduce the dimension and the complexity of Massive MIMO channel.

The hybrid structure can show itself in the precoded signal vector $\mathbf{x}_n$ expression. As in the Joint Spatial Division Multiplexing (JSDM) framework given in [11], the precoded signal vector at time index n can be defined as

$$\mathbf{x}_n = \mathbf{B}\,\mathbf{F}(\{\mathbf{d}_n\}) \tag{3.1}$$

where $\mathbf{d}_n$ is the $K \times 1$ desired signal vector that is wanted to be transmitted to all

groups with $\mathbb{E}\left\{\mathbf{d}_n \mathbf{d}_{n-l}^H\right\} = \mathbf{I}_K \delta_l$ and $\mathbf{d}_n$ is shown as

$$\mathbf{d}_n = \begin{bmatrix} \mathbf{d}_n^{(1)} \\ \mathbf{d}_n^{(2)} \\ \vdots \\ \mathbf{d}_n^{(G)} \end{bmatrix} \tag{3.2}$$

where each $\mathbf{d}_n^{(g)}$ is the $K_g \times 1$ desired signal vector for only group g user terminals at time index n. $\mathbf{F}()$ is digital precoder matrix operator that takes the desired signal vectors of all groups as input. By the proposed techniques, the inter-symbol interference (ISI) is completely eliminated in digital precoder side.

$\mathbf{B}$ is the analog beamforming matrix. Inter-group interference suppression from the signal is carried out by the analog beamforming stage of the system. The analog beamforming matrix $\mathbf{B}$ is constructed as

$$\mathbf{B} \triangleq \begin{bmatrix} \mathbf{S}^{(1)} & \mathbf{S}^{(2)} & \dots & \mathbf{S}^{(G)} \end{bmatrix}_{N \times D} \tag{3.3}$$

where $D = \sum_{g=1}^{G} D_g$ is the total RF chain number at BS and D_g is the number of RF chains allocated for group g user terminals and each $\mathbf{S}^{(g)}$ is the $N \times D_g$ analog beamforming matrix that reduces the dimension of MIMO channel for group g user terminals via proper spatial processing after digital to analog conversions. By this way, an effective channel is created and a performance close to that of the fully digital precoder can be achieved by using less RF chain components which makes the system more power efficient and less complex. Each $\mathbf{S}^{(g)}$ is created according to the analog beamforming type used in the system. These analog beamforming type options are explained in Section 3.2.3.

$\mathbf{F}()$ is the digital precoder matrix operator and can be expressed as

$$\mathbf{F}(\{\mathbf{d}_n\}) \triangleq \sum_{l=0}^{L-1} \mathrm{bdiag}\left\{\sqrt{c^{(g)}}\, \mathbf{W}_l^{(g)}\right\}_{g=1}^{G} \mathbf{d}_{n+l} \tag{3.4}$$

where $c^{(g)}$ is the power scaling factor to set the downlink channel power scale for each

group algorithmically and $\mathbf{W}_l^{(g)}$ is the digital precoding filter that can be changed according to the digital precoder type of the system. These digital precoder options are investigated in Section 3.3.2. The details of these definitions are explained in the subsections. The proposed beamforming architecture is the hybrid beamforming because the data is precoded with both analog and digital domains. Also, there are several selection options on setting the power scaling factor $c^{(g)}$ and they are expressed in Section 3.3.1.

A general picture of the proposed hybrid beamforming architecture can be seen in Figure 3.1 as block diagrams.

3.2 Analog Beamformer Design

The signal is converted to the analog signal after the desired signal $\mathbf{d}_n^{(g)}$ passes through the digital precoder, digital to analog converters and RF chains. At this point, the analog beamforming matrices $\mathbf{S}^{(g)}$ are created for all groups. To do this, long-term channel parameters such as CCMs $\mathbf{R}_l^{(g)}$ of all groups after user grouping are utilized. CCM information is obtained from 'Long Term Joint Angle Delay Power Profile Construction' unit and user grouping algorithm that can be seen in Figure 3.1. The details of the user grouping algorithm are investigated in Chapter 5.

3.2.1 Received Signal Model for Uplink Training Data Transmission in TDD Mode

Before the analog beamformer stage and the user grouping algorithm, the channel state information should be obtained and the channel covariance matrices of each user terminal should all be estimated. CSI is obtained in uplink training data transmission in TDD mode. The received signal at BS should be defined for uplink training mode as

$$\mathbf{y}_n = \sum_{g=1}^{G} \sum_{l=0}^{L-1} \mathbf{H}_l^{(g)} \mathbf{x}_{n-l}^{(g)} + \mathbf{n}_n \tag{3.5}$$

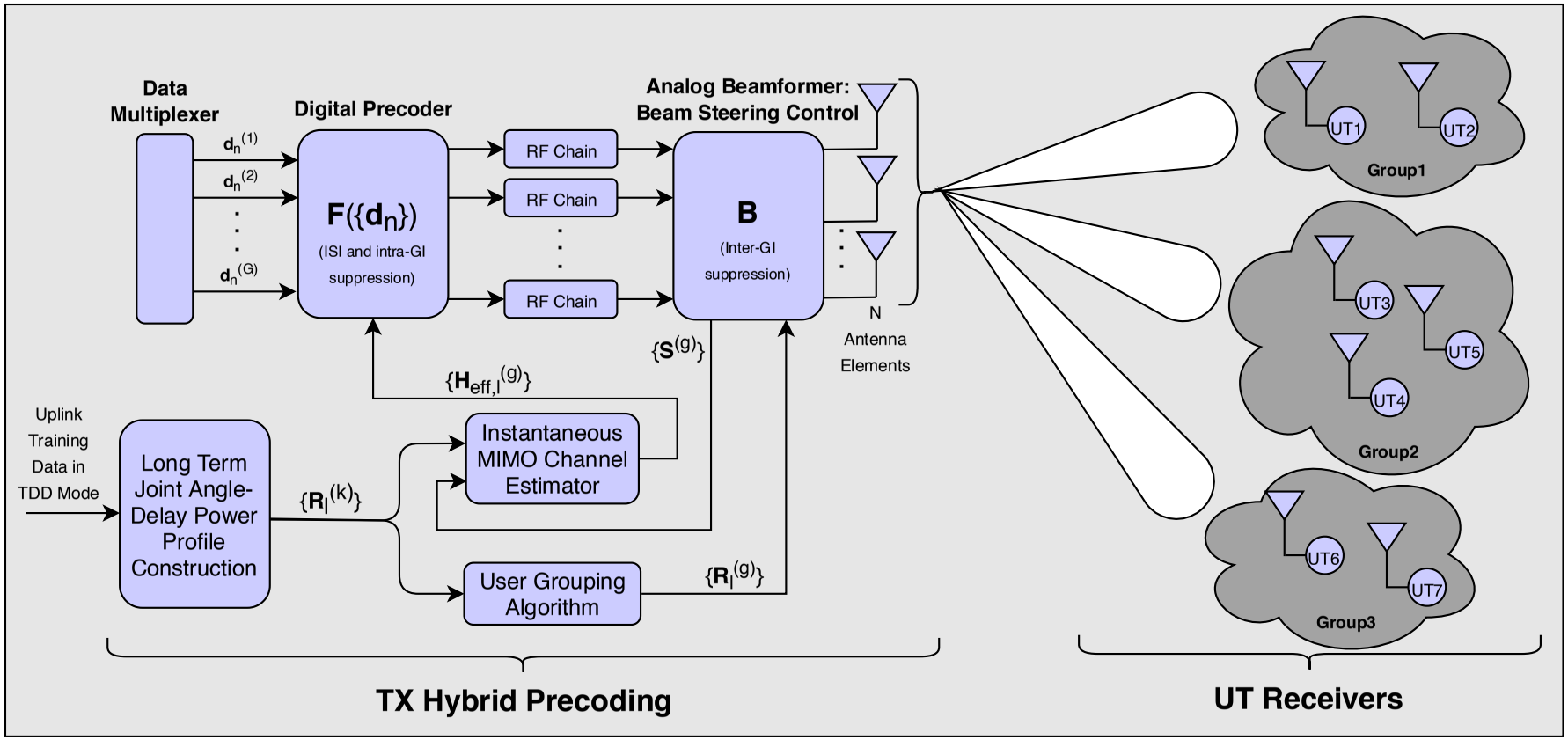

Figure 3.1: Proposed Hybrid Beamforming Architecture

where the training vectors are generated with the covariance matrix

$$\mathbb{E}\left\{\mathbf{x}_n^{(g)}\left(\mathbf{x}_m^{(g')}\right)^H\right\} = \frac{E_s^{(g)}}{K_g}\mathbf{I}_{K_g}\delta_{g-g'}\delta_{n-m} \tag{3.6}$$

so that $\mathbb{E}\left\{\|\mathbf{x}_n^{(g)}\|^2\right\} = E_s^{(g)}$ (by assuming equal transmit power among the users in the same group) where $E_s^{(g)}$ is the transmit power for group g user terminals and it is described in the digital stage of the hybrid structure.

We define a new covariance matrix $\mathbf{R}_\mathbf{y}$ of the received signal at BS for uplink training mode as

$$\mathbf{R}_\mathbf{y} = \mathbb{E}\left\{\mathbf{y}_n\left(\mathbf{y}_n\right)^H\right\} \tag{3.7}$$

By substituting Eqn. (3.5) into Eqn. (3.7),

$$\mathbf{R}_\mathbf{y} = \mathbb{E}\left\{\left(\sum_{g=1}^{G}\sum_{l=0}^{L-1}\mathbf{H}_l^{(g)}\mathbf{x}_{n-l}^{(g)} + \mathbf{n}_n\right)\left(\sum_{g=1}^{G}\sum_{l=0}^{L-1}\mathbf{H}_l^{(g)}\mathbf{x}_{n-l}^{(g)} + \mathbf{n}_n\right)^H\right\} \tag{3.8}$$

where the signal and the noise are uncorrelated so that the following equation emerges

$$\mathbf{R}_\mathbf{y} = \sum_{g=1}^{G}\sum_{l=0}^{L-1}\mathbb{E}\left\{\mathbf{H}_l^{(g)}\mathbf{x}_{n-l}^{(g)}\left(\mathbf{x}_{n-l}^{(g)}\right)^H\left(\mathbf{H}_l^{(g)}\right)^H\right\} + N_0\mathbf{I}_N \tag{3.9}$$

where N_0 is the noise power and

$$\mathbf{R}_\mathbf{y} = \sum_{g=1}^{G}\frac{E_s^{(g)}}{K_g}\sum_{l=0}^{L-1}\sum_{k=1}^{K_g}\mathbf{R}_l^{(g_k)} + N_0\mathbf{I}_N \tag{3.10}$$

by using the fact that

$$\mathbb{E}\left\{\mathbf{H}_l^{(g)}\left[\mathbf{H}_l^{(g)}\right]^H\right\} = \sum_{k=1}^{K_g}\mathbf{R}_l^{(g_k)} \tag{3.11}$$

As can be seen in Eqn. (3.10), $\mathbf{R_y}$ contains all channel covariance matrices for all MPCs of all user terminals in the system. It also contains the noise term. The covariance matrix $\mathbf{R_y}$ will be used to suppress the inter-group interference in the generalized type eigen beamformers that are shown in Subsections 3.2.3.4 and 3.2.3.5.

3.2.2 Channel Covariance Matrix Construction After User Grouping

In order to create the beams for all groups, the user terminals should be partitioned into the groups first, by the user grouping algorithm. After the user terminals are grouped via the algorithm, group channel covariance matrix $\mathbf{R}_l^{(g)}$ that is uniform for all user terminals in group g is constructed by adding all channel covariance matrices of the user terminals in group g and can be shown mathematically as

$$\mathbf{R}_l^{(g)} = \sum_{k=1}^{K_g} \mathbf{R}_l^{(g_k)} \tag{3.12}$$

Some of the analog beamformer types use all the multi-path components of the desired group that the analog beamforming matrix is created for. For this purpose, a new covariance matrix sum should be created in order to contain all the intra-group channel covariance matrix information of the multi-path components in one matrix. This matrix can be stated as

$$\mathbf{R}_{sum}^{(g)} \triangleq \sum_{l=0}^{L_g-1} \mathbf{R}_l^{(g)} \tag{3.13}$$

where Eqn. (3.12) is substituted into Eqn. (3.13) and the following equation is found as

$$\mathbf{R}_{sum}^{(g)} \triangleq \sum_{l=0}^{L_g-1} \sum_{k=1}^{K_g} \mathbf{R}_l^{(g_k)} \tag{3.14}$$

3.2.3 Analog Precoding Techniques

After the digital precoder type is selected, five different types of the analog beamformer are investigated. Seeing the differences of these five different analog beamformer types and comparing them with each other are the best way to find the optimum analog beamformer and to see how changes affect the performance result. For the following five analog beamformer types, the analog beamforming matrix $\mathbf{S}^{(g)}$ for group g can be designed as

$$\mathbf{S}^{(g)} = \begin{bmatrix} \mathbf{S}^{(g)}(0) & \mathbf{S}^{(g)}(1) & \dots & \mathbf{S}^{(g)}(L_g - 1) \end{bmatrix} \tag{3.15}$$

where $\mathbf{S}^{(g)}(l)$ is a $N \times d_l^{(g)}$ matrix of the analog beamforming matrix for the l^{th} multi-path component of the group g user terminals, $d_l^{(g)}$ is the number of RF chains allocated for the l^{th} multi-path component of the group g user terminals and $\sum_{l=0}^{L_g-1} d_l^{(g)} = D_g$. The design of $\mathbf{S}^{(g)}(l)$ changes according to the chosen analog beamforming type.

For a given digital precoder type, the following five analog beamformer types are investigated throughout the research.

3.2.3.1 Conventional DFT Beamformer

For a given MPC number L_g, the RF chains reserved for group g user terminals are shared equally among all MPCs. If the total RF chains reserved for group g user terminals are divided and there are remainders, the remainders are randomly distributed to the MPCs of group g user terminals. Let the number of RF chains for group g user terminals is D_g. For the l^{th} multi-path component of group g, $\mathbf{S}^{(g)}(l)$ is defined as Eqn. (3.16) if conventional DFT beamformer is chosen.

$$\mathbf{S}^{(g)}(l) = \begin{bmatrix} \mathbf{a}(\theta_0) & \mathbf{a}(\theta_1) & \mathbf{a}(\theta_2) & \dots & \mathbf{a}(\theta_{d_l^{(g)}-1}) \end{bmatrix} \tag{3.16}$$

where $\mathbf{a}(\theta)$ is the unit norm steering vector for an azimuth angle θ. That is, the columns of the analog beamforming matrix are the unit norm steering vectors if conventional DFT beamformer is used. Thus, the beamformer does not exploit the channel covariance matrices, it just uses the steering vectors that are created in the angular

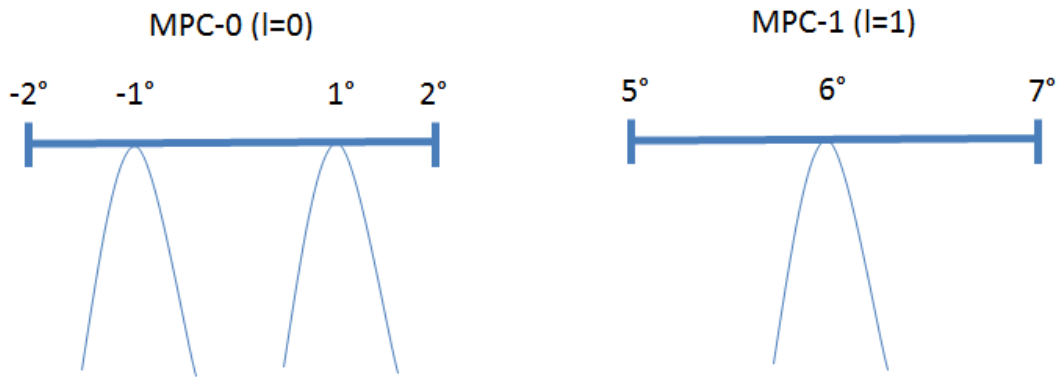

Figure 3.2: DFT Beam Distribution Visualization

sectors of MPCs.

The azimuth angles in Eqn. (3.16) can be analytically found as

$$\begin{aligned} \theta_0 &= \theta_{l,min}^{(g)} + \frac{\Delta\theta_l^{(g)}}{2d_l^{(g)}}, & \theta_1 &= \theta_0 + \frac{\Delta\theta_l^{(g)}}{d_l^{(g)}} \\ \theta_2 &= \theta_1 + \frac{\Delta\theta_l^{(g)}}{d_l^{(g)}}, & \theta_{d_l^{(g)}-1} &= \theta_{d_l^{(g)}-2} + \frac{\Delta\theta_l^{(g)}}{d_l^{(g)}} \end{aligned} \tag{3.17}$$

where $\Delta\theta_l^{(g)} = \theta_{l,max}^{(g)} - \theta_{l,min}^{(g)}$.

For example, to understand the beam distribution better, a random scenario is created. In this scenario, there are two MPCs with $\theta_{0,min}^{(g)} = -2$, $\theta_{0,max}^{(g)} = 2$ and $d_0^{(g)} = 2$ for MPC-0 ($l = 0$) and $\theta_{1,min}^{(g)} = 5$, $\theta_{1,max}^{(g)} = 7$ and $d_1^{(g)} = 1$ for MPC-1 ($l = 1$) in group g. For this scenario, the beams are distributed to each angular sectors of the multi-path components like in Figure 3.2.

3.2.3.2 Angle Only Eigen Beamformer (AO-EB)

In this analog beamformer type, the first D_g dominant eigenvectors of $\mathbf{R}_{sum}^{(g)}$ are chosen as the columns of $\mathbf{S}^{(g)}$, as given in Eqn. (3.18). In other words, the analog beamformer is only interested in the total channel covariance matrix $\mathbf{R}_{sum}^{(g)}$ information, it does not consider any other multi-path component, seperately. That is, it does not take the delay terms into account. That is why this analog beamformer is called

'angle only', not 'joint angle-delay'. Because it does not give an importance to the multi-path components and it does not use the parameter $\mathbf{R_y}$, the beamformer can not suppress the undesired multi-path components coming from different groups other than the desired one. As a result of this, the inter-group interference in the signal makes it hard to detect the desired group signal if there exists a considerable transmit power given to the undesired groups. The beam is steered to the all multi-path components in the group of interest. Because it uses the sum of the channel covariance matrices of the multi-path components in the desired group, creating the analog beamforming matrix $\mathbf{S}^{(g)}$ directly is meaningful instead of creating each column matrices $\mathbf{S}^{(g)}(l)$ of $\mathbf{S}^{(g)}$, seperately. That is, a resulting analog beamforming matrix $\mathbf{S}^{(g)}$ is created by using total RF chains allocated for the group of interest. It is not formed by dividing the matrix $\mathbf{S}^{(g)}$ into the column matrices and by creating the column matrices of $\mathbf{S}^{(g)}$, seperately. Therefore, there comes also an interference coming from the MPC's of the group of interest, in addition to the inter-group interference. Nevertheless, compared to the conventional DFT beamformer, this beamformer type gives better performance results since it exploits the second order statistics (channel covariance matrices) instead of using only unit norm steering vectors.

$$\mathbf{S}^{(g)} = eigs(\mathbf{R}^{(g)}_{sum}, D_g) \tag{3.18}$$

3.2.3.3 Joint Angle-Delay Eigen Beamformer (JAD-EB)

In addition to the angle only eigen beamformer, joint angle-delay eigen beamformer investigates each multi-path component in the group of interest, seperately. Thus, this type of analog beamformer is designed by choosing the column matrices $\mathbf{S}^{(g)}(l)$ of the analog beamforming matrix $\mathbf{S}^{(g)}$ as the first $d_l^{(g)}$ dominant eigenvectors of $\mathbf{R}_l^{(g)}$ for the l^{th} multi-path component as in Eqn. (3.19).

$$\mathbf{S}^{(g)}(l) = eigs(\mathbf{R}_l^{(g)}, d_l^{(g)}) \tag{3.19}$$

where all column matrices are combined and Eqn. (3.15) is obtained as follows

$$\mathbf{S}^{(g)} = \begin{bmatrix} \mathbf{S}^{(g)}(0) & \mathbf{S}^{(g)}(1) & \dots & \mathbf{S}^{(g)}(L_g - 1) \end{bmatrix} \tag{3.20}$$

As in the DFT beamformer case, the RF chains reserved for group g user terminals are shared equally among all MPCs. The joint angle-delay eigen beamformer (JAD-EB) can show a better performance than the previous angle only eigen beamformer (AO-EB) because it creates seperate beams for different multi-path components in the group of interest. Therefore, ISI can be eliminated by creating seperate beams for different multi-path components. However, the intergroup interference still exists since this beamformer does not still use the parameter $\mathbf{R_y}$ to suppress the multi-path components of the undesired groups by creating the generalized eigenspaces.

3.2.3.4 Angle Only Generalized Eigen Beamformer (AO-GEB)

In the first three analog beamformer types, the inter-group interference is not considered and therefore, they cannot suppress the undesired signal coming from other group users. Angle only generalized eigen beamformer (AO-GEB) is promising because it takes the inter group interference into account by using the parameter $\mathbf{R_y}$ and tries to suppress it by choosing the first D_g dominant generalized eigenvectors of $\mathbf{R}_{sum}^{(g)}$ and $\mathbf{R_y}$ like in Eqn. (3.21). In order to obtain a nearly interference free analog beamformer, this beamformer is not the optimal one. It can eliminate the inter-group interference, but it still suffers from the inter-symbol interference (ISI) because a uniform beam is steered to the group. This beam does not consider the multi-path components of the desired group, seperately, so it does not take the delay terms into account like angle only eigen beamformer (AO-EB). The next solution can be using joint angle-delay plane together with creating generalized eigenspaces like joint angle-delay generalized eigen beamformer (JAD-GEB).

$$\mathbf{S}^{(g)} = eigs(\mathbf{R}_{sum}^{(g)}, \mathbf{R_y}, D_g) \tag{3.21}$$

3.2.3.5 Joint Angle-Delay Generalized Eigen Beamformer (JAD-GEB)

Lastly, the proposed analog beamformer type in the hybrid beamforming structure is the joint angle-delay generalized eigen beamformer (JAD-GEB). In this type, the delay terms are also considered, in addition to the angle terms. By creating the beams

using the generalized eigenspaces, the MPCs other than the desired one can be suppressed. Among all the MPCs in group g, the RF chains reserved for group g users are distributed through an algorithm that finds the best intra-group RF chain distribution that maximizes a metric consisting of generalized eigenvalues of the terms in Eqn. (3.22). Inter-group and intra-group RF chain distribution is particularly mentioned in Section 3.2.4. It is constructed as the first $d_l^{(g)}$ dominant generalized eigenvectors of $\mathbf{R}_l^{(g)}$ and $\mathbf{R}_\mathbf{y}$ as

$$\mathbf{S}^{(g)}(l) = eigs(\mathbf{R}_l^{(g)}, \mathbf{R}_\mathbf{y}, d_l^{(g)}) \tag{3.22}$$

where all column matrices are combined and Eqn. (3.15) is obtained as

$$\mathbf{S}^{(g)} = \left[\begin{array}{cccc} \mathbf{S}^{(g)}(0) & \mathbf{S}^{(g)}(1) & \dots & \mathbf{S}^{(g)}(L_g - 1) \end{array} \right] \tag{3.23}$$

The proposed analog beamformer type is structured based on the pre-processing technique in [24], where the optimality was demonstrated for several different criterion. The scheme in [24] is modified such that the orthogonality between the eigenspaces of different MPCs in reduced dimension is guaranteed by taking both inter-group interference and ISI into account. Therefore, there is no need for equalization to mitigate ISI in digital domain (after analog beamforming); just channel matched filtering in reduced dimension is sufficient to attain ISI-free samples and full multi-path diversity.

3.2.4 RF Chain Distribution

RF chain distribution is crucial for the proposed reduced dimensional hybrid precoder structure. It plays a critical role for the performance of the precoder since the system has a few RF chains compared to the antenna number. The RF chain distribution is firstly applied between the groups, this type of RF chain distribution is named as intergroup RF chain distribution among MPCs. There is also an RF chain distribution among MPCs in the same group in the proposed joint angle-delay generalized eigenbeamformer (JAD-GEB). It is named as intra-group RF chain distribution. Both RF

chain distributions are described in the subsections.

3.2.4.1 Inter-group RF Chain Distribution

After user terminals are divided into multiple groups through the user grouping algorithm, RF chain distribution is required to create the beams for each group in analog beamformer part of the hybrid structure. If the system has enough RF chains to support all multi-path components of all user terminals, they can be shared to the groups equally without any performance loss. However, since the system does not have enough number of RF chains, RF chain distribution becomes crucial for the beam creation and the performance of the beamformer. Therefore, two types of smart distributions based on the user number and the multi-path component number of the groups are proposed to maximize the channel capacity performance.

First, the number of RF chains allocated for group g user terminals D_g can be distributed as

$$D_g = max\{K_g, L_g\} \tag{3.24}$$

where total RF chain number $D = \sum_{g=1}^{G} D_g$ in the system has a lower bound of

$$D \geqslant \sum_{g=1}^{G} max\{K_g, L_g\} \tag{3.25}$$

If the total RF chain number D is equal to the boundary in Eqn. (3.25), the distribution to the groups is completed as in Eqn. (3.24). If it exceeds the boundary, the remaining RF chains after the distribution to the groups like in Eqn. (3.24) are distributed starting from the group that has the maximum $max\{K_g, L_g\}$ value among all groups. An example scenario like in Table 3.1 can be investigated to understand the distribution better. In this scenario, the total RF chain number D in the system cannot be lower than $\sum_{g=1}^{G} max\{K_g, L_g\} = 8$. Let $D = 10$ to see the remaining distribution case clearly. The first distribution is done by applying Eqn. (3.24) and the column with title 'D_g (withoutremaining)' shows the results. After the first distribution, the

remaining two RF chains are distributed to group 2 and group 3, one by one since they have maximum value of $max\{K_g, L_g\}$ compared to group 1. Finally, the RF chain distribution to the groups can be seen in the column named as 'final D_g'.

Table 3.1: Example Scenario for the First Type of Inter-group RF Chain Distribution

Group Number	K_g	L_g	D_g (withoutremaining)	final D_g
1	2	1	$max\{2,1\} = 2$	2
2	1	3	$max\{1,3\} = 3$	4
3	3	2	$max\{3,2\} = 3$	4

As the second smart distribution type, the total RF chain number D can be shared to the groups according to their number of user terminals. That is, $D_g = K_g$. After every user has more than one RF chain, if there are some remaining RF chains, they are distributed to the user terminals one by one. An example distribution of this smart distribution type for the scenario given in the previous paragraph is shown in Table 3.2.

Table 3.2: Example Scenario for the Second Type of Inter-group RF Chain Distribution

Group Number	K_g	L_g	D_g (withoutremaining)	final D_g
1	2	1	2	4
2	1	3	1	3
3	3	2	3	4

3.2.4.2 Intra-group RF Chain Distribution

After the inter-group RF chain distribution is completed, in some analog beamformer types, a smart intra-group RF chain distribution is also necessary. The analog beamformers like angle only eigen beamformer (AO-EB) and angle only generalized eigen beamformer (AO-GEB) do not need any intra-group RF chain distribution since they create a single beam by using all RF chains D_g reserved for the group of interest. They do not consider the delay terms differently. On the other hand, the proposed

joint angle-delay generalized eigen beamformer needs a smart RF chain distribution for the maximum performance. A generalized eigenvalue based smart intra-group RF chain distribution is proposed to find the optimal intra-group RF chain distribution Λ so that

$$\Lambda = \arg \max_{d_l^{(g)}, D_g = \sum_{l=0}^{L_g-1} d_l^{(g)}} \prod_{l=0}^{L_g-1} \prod_{n=1}^{d_l^{(g)}} (1 + \lambda_{l,n}^{(g)}) \tag{3.26}$$

where $\lambda_{l,n}^{(g)}$ is the n^{th} generalized eigenvalue of the term in Eqn. (3.23). The final distribution has the maximum metric value.

3.3 Digital Precoder Design

As can be seen in Figure 3.1, the desired signals $\mathbf{d}_n^{(g)}$'s firstly pass through the digital precoder. As stated earlier, the digital precoder is mathematically defined as

$$\mathbf{F}(\{\mathbf{d}_n\}) \triangleq \sum_{l=0}^{L-1} \mathrm{bdiag} \left\{ \sqrt{c^{(g)}}\, \mathbf{W}_l^{(g)} \right\}_{g=1}^{G} \mathbf{d}_{n+l} \tag{3.27}$$

where $c^{(g)}$ is the power scaling factor and it determines how the transmit power will be distributed to each group. It can be selected algorithmically with two different options which are per group power constraint and total group power constraint. In addition to the transmit power distribution, there are two different structures for the digital precoding filter $\mathbf{W}_l^{(g)}$. In both of the digital precoding techniques, the precoder takes the effective reduced dimensional channel estimation as an input. The effective reduced dimensional channel, i.e., the channel after analog beamforming is estimated for all user terminals in TDD mode in 'Instantaneous MIMO Channel Estimator' unit in Figure 3.1. By knowing the instantaneous channel state information, the effective reduced dimensional channel $\mathbf{H}_{eff,l}^{(g',g)}$ for all MPCs can be expressed as

$$\mathbf{H}_{eff,l}^{(g',g)} \triangleq \left[\mathbf{S}^{(g')} \right]^H \mathbf{H}_l^{(g)} \tag{3.28}$$

This effective channel is utilized in the digital precoder design with the advantage of reduced complexity. Before going into the detailed information on the digital precoder design, the power scaling factor setting by the transmit power constraints is investigated.

3.3.1 Transmit Power Constraint

The power scaling factor $c^{(g)}$ can be calculated in two different ways according to the two power constraints. One of them is the total power constraint or the joint group processing and the other one is the per group power constraint or per group processing.

3.3.1.1 Total Power Constraint

The first power constraint to set the power scaling factors $c^{(g)}$ is the total power constraint or the joint group processing. According to the total power constraint, all $c^{(g)}$'s are equal for all groups. That is, $c^{(g)} = c = \text{constant}$. It physically means that BS gives the same power to all groups without considering any other changes between the groups.

3.3.1.2 Per Group Power Constraint

The second constraint is the per group power constraint (per group processing). With this constraint, BS tries to balance the power difference between the groups by transmitting less power to the closer group. This difference comes from the different distances of the groups to BS. The detailed mathematical analysis can be seen in Section 3.3.1.3.

3.3.1.3 The Power Scaling Factor Calculation

To find a mathematical expression for $c^{(g)}$, the expectation value of norm square of the precoded signal vector or the total transmit power $\mathbb{E}\{\|\mathbf{x}_n\|^2\} = E_s$ should be

found firstly as

$$\mathrm{SNR}_{\mathrm{TX}} = \frac{E_s}{N_0} = \frac{\mathbb{E}\left\{\|\mathbf{x}_n\|^2\right\}}{N_0} = \frac{\mathrm{Tr}\left\{\mathbb{E}\left\{\mathbf{x}_n\mathbf{x}_n^H\right\}\right\}}{N_0} \tag{3.29}$$

where $\mathrm{SNR}_{\mathrm{TX}}$ is the transmit SNR. The expression at Eqn. (3.29) are modified as

$$\frac{\mathrm{Tr}\left\{\mathbb{E}\left\{\mathbf{x}_n\mathbf{x}_n^H\right\}\right\}}{N_0} = \frac{\mathrm{Tr}\left\{\mathbf{B}\,\mathbf{R_F}\mathbf{B}^H\right\}}{N_0} \tag{3.30}$$

where

$$\mathbf{R_F} = \mathbb{E}\left\{\mathbf{F}\left(\{\mathbf{d}_n\}\right)\mathbf{F}^H\left(\{\mathbf{d}_n\}\right)\right\} \tag{3.31}$$

where $\mathbf{R_F}$ can be expanded as

$$\mathbf{R_F} = \sum_{l_1=0}^{L-1}\sum_{l_2=0}^{L-1}\mathrm{bdiag}\left\{c^{(g)}\mathbb{E}\left\{\mathbf{W}_{l_1}^{(g)}\left[\mathbf{W}_{l_2}^{(g)}\right]^H\right\}\right\}_{g=1}^{G}\delta_{l_1-l_2} \tag{3.32}$$

By substituting Eqn. (3.32) into Eqn. (3.30), the following expression is obtained as

$$\frac{\mathbb{E}\left\{\|\mathbf{x}_n\|^2\right\}}{N_0} = \frac{\mathrm{Tr}\left\{\mathbf{B}\,\mathbf{R_F}\mathbf{B}^H\right\}}{N_0} \tag{3.33}$$

and

$$\frac{\mathbb{E}\left\{\|\mathbf{x}_n\|^2\right\}}{N_0} = \frac{1}{N_0}\sum_{g=1}^{G}c^{(g)}\underbrace{\sum_{l=0}^{L-1}\mathrm{Tr}\left\{\mathbf{S}^{(g)}\mathbb{E}\left\{\mathbf{W}_l^{(g)}\left[\mathbf{W}_l^{(g)}\right]^H\right\}\left[\mathbf{S}^{(g)}\right]^H\right\}}_{\triangleq P^{(g)}} \tag{3.34}$$

where

$$P^{(g)} \triangleq \sum_{l=0}^{L-1}\mathrm{Tr}\left\{\mathbf{S}^{(g)}\mathbb{E}\left\{\mathbf{W}_l^{(g)}\left[\mathbf{W}_l^{(g)}\right]^H\right\}\left[\mathbf{S}^{(g)}\right]^H\right\} \tag{3.35}$$

where $\frac{1}{N_0} = \mathrm{SNR}_{uplink}$ since the desired signal vectors are unit variance and uncorrelated to each other. $P^{(g)}$ is a deterministic parameter and it can be calculated with the knowledge of the analog beamforming matrix and the digital precoding matrix of the group of interest. To find a final expression,

$$\mathrm{SNR}_{TX} = \frac{\mathbb{E}\left\{\|\mathbf{x}_n\|^2\right\}}{N_0} = \frac{E_s}{N_0} = \frac{1}{N_0} \sum_{g=1}^{G} c^{(g)} P^{(g)} \tag{3.36}$$

where total transmit power $E_s = \mathbb{E}\left\{\|\mathbf{x}_n\|^2\right\}$ given to the system containing all groups can be expressed as

$$E_s = \sum_{g=1}^{G} c^{(g)} P^{(g)} = \sum_{g=1}^{G} E_s^{(g)} \tag{3.37}$$

The transmit power allocated to the group g user terminals is $E_s^{(g)} = \mathbb{E}\left\{\|\mathbf{x}_n^{(g)}\|^2\right\} = c^{(g)} P^{(g)}$ and it is assumed that the power is distributed equally among all user terminals in the same group. The total transmit power is defined as in Eqn. (3.37). Since $\mathrm{SNR}_{\mathrm{TX}} = E_s/N_0$, $c^{(g)}$ should be selected as

$$c^{(g)} = E_s^{(g)}/P^{(g)} \tag{3.38}$$

where The transmit power for the group g user terminals $E_s^{(g)}$ is

$$E_s^{(g)} = \begin{cases} \dfrac{E_s P^{(g)}}{\sum_{g=1}^{G} P^{(g)}} & \text{for total power constraint} \\ \dfrac{E_s}{G} & \text{for per group power constraint} \end{cases} \tag{3.39}$$

3.3.2 Digital Precoding Techniques

For a given analog beamforming structure, following two types can be constructed for the digital precoding filter $\mathbf{W}_l^{(g)}$.

3.3.2.1 Channel Matched Filter (CMF) Type Precoder

It is simply a channel matched filter. For this case, $\mathbf{W}_l^{(g)}$ is equal to the effective reduced dimensional channel matrix for $g' = g$ and can be shown as

$$\mathbf{W}_l^{(g)} \triangleq \mathbf{H}_{eff,l}^{(g,g)} \tag{3.40}$$

If CMF type precoder is selected as the digital precoder of the system, we can analytically find an expression for $P^{(g)}$. Eqn. (3.40) is substituted into Eqn. (3.35) as

$$P^{(g)} = \sum_{l=0}^{L-1} \mathrm{Tr}\left\{ \mathbf{S}^{(g)} \, \mathbf{R}_{\mathbf{H}_{eff,l}^{(g,g)}} \left[\mathbf{S}^{(g)}\right]^H \right\} \tag{3.41}$$

where

$$\mathbf{R}_{\mathbf{H}_{eff,l}^{(g,g)}} \triangleq \mathbb{E}\left\{ \mathbf{H}_{eff,l}^{(g,g)} \left[\mathbf{H}_{eff,l}^{(g,g)}\right]^H \right\} \tag{3.42}$$

By substituting the effective channel matrix $\mathbf{H}_{eff,l}^{(g,g)}$ for $g' = g$ into Eqn. (3.42),

$$\mathbf{R}_{\mathbf{H}_{eff,l}^{(g,g)}} = \left[\mathbf{S}^{(g)}\right]^H \mathbb{E}\left\{ \mathbf{H}_l^{(g)} \left[\mathbf{H}_l^{(g)}\right]^H \right\} \mathbf{S}^{(g)} \tag{3.43}$$

where the expectation value of the covariance matrix of the instantaneous channel matrix is

$$\mathbb{E}\left\{ \mathbf{H}_l^{(g)} \left[\mathbf{H}_l^{(g)}\right]^H \right\} = \sum_{k=1}^{K_g} \mathbf{R}_l^{(g_k)} \tag{3.44}$$

Then, for CMF type precoder, we analytically find $P^{(g)}$ as

$$P^{(g)} = \sum_{k=1}^{K_g} \sum_{l=0}^{L-1} \mathrm{Tr}\left\{ \mathbf{S}^{(g)} \left[\mathbf{S}^{(g)}\right]^H \mathbf{R}_l^{(g_k)} \mathbf{S}^{(g)} \left[\mathbf{S}^{(g)}\right]^H \right\} \tag{3.45}$$

3.3.2.2 Channel Matched Filter-Spatial Zero Forcing (CMF-SZF) Type Precoder

If this precoder type is selected as the digital precoder, $\mathbf{W}_l^{(g)}$ can be designed as

$$\mathbf{W}_l^{(g)} \triangleq \mathbf{H}_{eff,l}^{(g,g)} \left(\sum_{m=0}^{L-1} \left[\mathbf{H}_{eff,m}^{(g,g)} \right]^H \mathbf{H}_{eff,m}^{(g,g)} + \frac{N_0}{E_s} \mathbf{I}_{K_g} \right)^{-1} \tag{3.46}$$

where $P^{(g)}$ can be calculated with the help of Monte Carlo Simulation for this type of the digital precoder. It is a regularized type CMF-SZF type precoder and the term N_0/E_s is named as the regularization constant.

If a proper analog beamformer that rejects inter-group interference and ISI is utilized, it can be said that $\mathbf{H}_{eff,l}^{(g',g)} = \mathbf{0}$ for $g' \neq g$. Since the eigenspaces of different MPCs are approximately orthogonal in a proper beamspace after analog beamforming, we get $\left(\mathbf{H}_{eff,l}^{(g,g)} \right)^H \left(\mathbf{H}_{eff,l'}^{(g,g)} \right) = \mathbf{0}$ for $l = l'$.

There is a reason that this precoder expression is chosen as the digital precoder part of the structure. For this purpose, let us remember the received signal at the user terminals as

$$\mathbf{y}_n^{(g)} = \sum_{l=0}^{L-1} [\mathbf{H}_l^{(g)}]^H \mathbf{B}\, \mathbf{F}(\{\mathbf{d}_{n-l}\}) + \mathbf{n}_n \tag{3.47}$$

where the analog beamforming and digital precoding matrices are substituted into the equation and a final received signal model is shown as

$$\mathbf{y}_n^{(g)} = \sum_{g'=1}^{G} \sum_{l=-(L-1)}^{L-1} \mathbf{R}_l^{(g',g)}\, \mathbf{d}_{n+l}^{(g')} + \mathbf{n}_n \tag{3.48}$$

where $\mathbf{R}_l^{(g',g)}$ can be defined as

$$\mathbf{R}_l^{(g',g)} \triangleq \sqrt{C^{(g')}} \sum_{m=0}^{L-1} \left(\mathbf{H}_{eff,m-l}^{(g',g)} \right)^H \mathbf{W}_m^{(g')} \tag{3.49}$$

If CMF-SZF type precoder is utilized as the digital precoder of the system and $\mathbf{W}_m^{(g')}$ expression in Eqn. (3.49) is substituted as in Eqn. (3.46), the received signal at the user terminals can be reduced as

$$\mathbf{y}_n^{(g)} \approx \sqrt{c^{(g)}}\, \mathbf{d}_{n+l}^{(g)} + \mathbf{n}_n \tag{3.50}$$

where the proposed digital precoder completely removes ISI and intra-group interference as shown in Eqn. (3.50) because undesired multi-path component terms are eliminated with the inverse term in the CMF-SZF type digital precoder expression in Eqn. (3.46).

CHAPTER 4

PERFORMANCE ANALYSIS BASED ON ACHIEVABLE INFORMATION RATE (AIR)

After defining the digital precoders and analog beamformers of the system at the base station, the performance of the hybrid structure is investigated through a capacity parameter that is the achievable information rate (AIR). AIR is calculated at the single antenna user terminals. Each user terminal receives a signal from all antennas at the base station.

4.1 Signal to Interference Noise Ratio (SINR) Calculation

To find a mathematical definition for AIR, signal to interference noise ratio (SINR) calculation should be operated. SINR can be calculated analytically if CMF type digital precoder is utilized while it is calculated with the help of Monte Carlo Simulation if CMF-SZF type digital precoder is used.

4.1.1 General SINR Expression

To find a general definition for SINR, let us modify Eqn. (2.1) by substituting Eqn. (3.1) into it as

$$\mathbf{y}_n^{(g)} = \sum_{l=0}^{L-1} [\mathbf{H}_l^{(g)}]^H \mathbf{B}\, \mathbf{F}(\{\mathbf{d}_{n-l}\}) + \mathbf{n}_n \tag{4.1}$$

If the matrices in Eqn. (4.1) are substituted,

$$\mathbf{y}_n^{(g)} = \sum_{l=0}^{L-1} \sum_{l'=0}^{L-1} \sum_{g'=1}^{G} \sqrt{c^{(g')}} \left(\mathbf{H}_{eff,l}^{(g',g)} \right)^H \mathbf{W}_{l'}^{(g')} \mathbf{d}_{n-l+l'}^{(g')} + \mathbf{n}_n \tag{4.2}$$

$$= \sum_{g'=1}^{G} \sum_{l=-(L-1)}^{L-1} \mathbf{R}_l^{(g',g)} \mathbf{d}_{n+l}^{(g')} + \mathbf{n}_n \tag{4.3}$$

where $\mathbf{R}_l^{(g',g)}$ can be defined as

$$\mathbf{R}_l^{(g',g)} \triangleq \sqrt{c^{(g')}} \sum_{m=0}^{L-1} \left(\mathbf{H}_{eff,m-l}^{(g',g)} \right)^H \mathbf{W}_m^{(g')} \tag{4.4}$$

Let the desired (intended) group is group g. After defining all parameters and definitions in $\mathbf{y}_n^{(g)}$, the received signal by the k^{th} user terminal in group g at time index n is defined as

$$r_n^{(g_k)} = \left(\mathbf{e}_k^{(g)} \right)^T \mathbf{y}_n^{(g)} \tag{4.5}$$

where $\mathbf{e}_k^{(g)}$ is a $K_g \times 1$ vector whose elements are all zero except the k^{th} entry. If $\mathbf{y}_n^{(g)}$ is substituted into Eqn. (4.5),

$$r_n^{(g_k)} = \sum_{g'=1}^{G} \sum_{l=-(L-1)}^{L-1} \left(\mathbf{e}_k^{(g)} \right)^T \mathbf{R}_l^{(g',g)} \mathbf{d}_{n+l}^{(g')} + \left(\mathbf{e}_k^{(g)} \right)^T \mathbf{n}_n \tag{4.6}$$

$$= \beta^{(g_k)} d_n^{(g_k)} + \xi_n^{(g_k)} \tag{4.7}$$

where $\beta^{(g_k)} \triangleq \left(\mathbf{e}_k^{(g)} \right)^T \mathbf{R}_0^{(g,g)} \mathbf{e}_k^{(g)}$ is called the desired (intended) signal gain. $d_n^{(g_k)}$ is the k^{th} element of $\mathbf{d}_n^{(g)}$ and is called the desired signal for the k^{th} user terminal of the group g. $\xi_n^{(g_k)}$ term includes AWGN and all other signals except the desired one. It is composed of the intra-group signals and inter-group signals as well as the noise term.

The received signal power by the k^{th} user terminal in group g at time index n is

$$\mathbb{E}\left\{ \left| r_n^{(g_k)} \right|^2 \right\} = \mathbb{E}\left\{ \left| d_n^{(g_k)} \right|^2 \right\} \mathbb{E}\left\{ \left| \beta^{(g_k)} \right|^2 \right\} + \mathbb{E}\left\{ \left| \xi_n^{(g_k)} \right|^2 \right\} \tag{4.8}$$

where $\mathbb{E}\left\{\left|d_n^{(g_k)}\right|^2\right\} = 1$ as stated earlier. The equation can be expanded as follows:

$$\mathbb{E}\left\{\left|r_n^{(g_k)}\right|^2\right\} = \sum_{g'=1}^{G} \sum_{l=-(L-1)}^{L-1} \left(\mathbf{e}_k^{(g)}\right)^T \mathbf{\Theta}_l^{(g',g)} \mathbf{e}_k^{(g)} + N_0 \tag{4.9}$$

where $\mathbf{\Theta}_l^{(g',g)} = \mathbb{E}\left\{\mathbf{R}_l^{(g',g)} \left[\mathbf{R}_l^{(g',g)}\right]^H\right\}$. From Eqn. (4.9), the power of the desired signal is

$$\mathbb{E}\left\{\left|\beta^{(g_k)}\right|^2\right\} = \left(\mathbf{e}_k^{(g)}\right)^T \mathbb{E}\left\{\mathbf{R}_0^{(g,g)} \mathbf{E}_{K,k} \left[\mathbf{R}_0^{(g,g)}\right]^H\right\} \mathbf{e}_k^{(g)} \tag{4.10}$$

where $\mathbf{E}_{K,k} = \mathbf{e}_k^{(g)} \left(\mathbf{e}_k^{(g)}\right)^T$. The power of the interference part can be calculated by subtracting the desired signal power from the received signal power. That is,

$$\mathbb{E}\left\{\left|\xi_n^{(g_k)}\right|^2\right\} = \mathbb{E}\left\{\left|r_n^{(g_k)}\right|^2\right\} - \mathbb{E}\left\{\left|\beta^{(g_k)}\right|^2\right\} \tag{4.11}$$

SINR is expressed as

$$\mathrm{SINR}^{(\mathrm{g_k})} = \frac{\mathbb{E}\left\{\left|\beta^{(g_k)}\right|^2\right\}}{\mathbb{E}\left\{\left|\xi_n^{(g_k)}\right|^2\right\}} \tag{4.12}$$

Therefore, once the desired signal power $\mathbb{E}\left\{\left|\beta^{(g_k)}\right|^2\right\}$ and the interference signal power $\mathbb{E}\left\{\left|\xi_n^{(g_k)}\right|^2\right\}$ are known, SINR values can be calculated from Eqn. (4.12). If CMF-SZF type precoder is used as the digital precoder of the system, the expectations can be found with the help of the Monte Carlo Simulation. However, if CMF type precoder is chosen as the digital precoder, the expectation values can be found analytically.

4.1.2 Analytical SINR Calculation for CMF Type Precoder

To find an analytical expression for the expectations by using CMF type precoder, a new $D_{g'}L \times K_g$ dimension matrix can be defined as

$$\mathbf{\Phi}^{(g',g)} \triangleq \left[\begin{array}{cccc} \left(\mathbf{H}_{eff,0}^{(g',g)}\right)^H & \left(\mathbf{H}_{eff,1}^{(g',g)}\right)^H & \dots & \left(\mathbf{H}_{eff,L-1}^{(g',g)}\right)^H \end{array} \right]^H \tag{4.13}$$

$$\triangleq \left[\begin{array}{cccc} \boldsymbol{\phi}_1^{(g',g)} & \boldsymbol{\phi}_2^{(g',g)} & \dots & \boldsymbol{\phi}_{K_g}^{(g',g)} \end{array} \right] \tag{4.14}$$

where $\boldsymbol{\phi}_k^{(g',g)}$ is defined as the k^{th} column vector of $\mathbf{\Phi}^{(g',g)}$ matrix and can be found as

$$\boldsymbol{\phi}_k^{(g',g)} = \left[\begin{array}{c} \left[\mathbf{S}^{(g')}\right]^H \mathbf{H}_0^{(g)}(:,k) \\ \left[\mathbf{S}^{(g')}\right]^H \mathbf{H}_1^{(g)}(:,k) \\ \vdots \\ \left[\mathbf{S}^{(g')}\right]^H \mathbf{H}_{L-1}^{(g)}(:,k) \end{array} \right] \tag{4.15}$$

since $\mathbf{H}_{eff,l}^{(g',g)} = \left[\mathbf{S}^{(g')}\right]^H \mathbf{H}_l^{(g)}$ as stated in Eqn. (3.28). To obtain a convenient expression,

$$\boldsymbol{\phi}_k^{(g',g)} = \mathrm{diag}\left\{ \left[\begin{array}{ccc} \left[\mathbf{S}^{(g')}\right]^H & \dots & \left[\mathbf{S}^{(g')}\right]^H \end{array} \right] \right\} \left[\begin{array}{c} \mathbf{H}_0^{(g)}(:,k) \\ \mathbf{H}_1^{(g)}(:,k) \\ \vdots \\ \mathbf{H}_{L-1}^{(g)}(:,k) \end{array} \right] \tag{4.16}$$

where the expression can be defined with a kronecker product as

$$\boldsymbol{\phi}_k^{(g',g)} = \left[\mathbf{I}_L \otimes \left[\mathbf{S}^{(g')}\right]^H \right] \left[\begin{array}{c} \mathbf{H}_0^{(g)}(:,k) \\ \mathbf{H}_1^{(g)}(:,k) \\ \vdots \\ \mathbf{H}_{L-1}^{(g)}(:,k) \end{array} \right] \tag{4.17}$$

Then, because $\mathbf{W}_l^{(g)} \triangleq \mathbf{H}_{eff,l}^{(g,g)}$ for CMF type precoder from Eqn. (3.40), $\mathbf{R}_l^{(g',g)}$ matrix becomes

$$\mathbf{R}_l^{(g',g)} = \sqrt{c^{(g')}} \left(\mathbf{\Phi}^{(g',g)}\right)^H \mathbf{Q}_l^{(g')} \mathbf{\Phi}^{(g',g')} \tag{4.18}$$

where the following matrices are defined as

$$\mathbf{Q}_l^{(g)} \triangleq \mathbf{T}_l \otimes \mathbf{I}_{D_g} \tag{4.19}$$

where $\mathbf{T}_l$ is an $L \times L$ matrix where $(m,n)^{th}$ entry is δ_{m-n+l}. It is important to note that

$$\left(\mathbf{e}_k^{(g)}\right)^T \mathbf{R}_l^{(g',g)} \left[\mathbf{R}_l^{(g',g)}\right]^H \mathbf{e}_k^{(g)} = c^{(g')} \sum_{m=1}^{K_{g'}} \Omega_l^{(g',g)}(k,m) \tag{4.20}$$

where $\Omega_l^{(g',g)}(k,m)$ can be identified as

$$\Omega_l^{(g',g)}(k,m) \triangleq \left| \left(\boldsymbol{\phi}_k^{(g',g)}\right)^H \mathbf{Q}_l^{(g')} \boldsymbol{\phi}_m^{(g',g')} \right|^2 \tag{4.21}$$

This relation can be substituted into Eqn. (4.9) as

$$\mathbb{E}\left\{\left|r_n^{(g_k)}\right|^2\right\} = \sum_{g'=1}^{G} c^{(g')} \sum_{l=-(L-1)}^{L-1} \sum_{m=1}^{K_{g'}} \mathbb{E}\left\{\Omega_l^{(g',g)}(k,m)\right\} + N_0 \tag{4.22}$$

After defining the received signal power $\mathbb{E}\left\{\left|r_n^{(g_k)}\right|^2\right\}$ according to the parameter $\mathbb{E}\left\{\Omega_l^{(g',g)}(k,m)\right\}$, the total interference signal power can be calculated as

$$\mathbb{E}\left\{\left|\xi_n^{(g_k)}\right|^2\right\} = \mathbb{E}\left\{\left|r_n^{(g_k)}\right|^2\right\} - \mathbb{E}\left\{\left|\beta^{(g_k)}\right|^2\right\} \tag{4.23}$$

where the desired signal power $\mathbb{E}\left\{\left|\beta^{(g_k)}\right|^2\right\}$ can be modified with the parameter $\mathbb{E}\left\{\Omega_l^{(g',g)}(k,m)\right\}$ as,

$$\mathbb{E}\left\{\left|\beta^{(g_k)}\right|^2\right\} = c^{(g)}\ \mathbb{E}\left\{\Omega_0^{(g,g)}(k,k)\right\} \tag{4.24}$$

The only parameter that should be known in order to calculate all $\mathrm{AIR}^{(g)}$ values analytically is $\mathbb{E}\left\{\Omega_l^{(g',g)}(k,m)\right\}$. By using Lemma 1 inspired by [29], $\mathbb{E}\left\{\Omega_l^{(g',g)}(k,m)\right\}$ can be found analytically.

Lemma 1 *Let* $\boldsymbol{x}$ *and* $\boldsymbol{y}$ *be* N *dimensional zero mean circularly symmetric complex Gaussian vectors and* $\boldsymbol{A}$ *is a real symmetric* $N \times N$ *matrix. With these definitions, following mathematical property can be stated as*

$$\mathbb{E}\left\{\left|\boldsymbol{x}^H\boldsymbol{A}\boldsymbol{y}\right|^2\right\} = \mathrm{Tr}\left(\boldsymbol{A}^H\boldsymbol{R}_{\boldsymbol{xx}}\boldsymbol{A}\boldsymbol{R}_{\boldsymbol{yy}}\right) + \mathrm{Tr}\left(\boldsymbol{A}\boldsymbol{R}_{\boldsymbol{yx}}\right)\ \mathrm{Tr}\left(\boldsymbol{A}^H\boldsymbol{R}_{\boldsymbol{xy}}\right) \tag{4.25}$$

where $\boldsymbol{R}_{\boldsymbol{xx}} = \mathbb{E}\left\{\boldsymbol{x}\boldsymbol{x}^H\right\}$, $\boldsymbol{R}_{\boldsymbol{yy}} = \mathbb{E}\left\{\boldsymbol{y}\boldsymbol{y}^H\right\}$ *and* $\boldsymbol{R}_{\boldsymbol{xy}} = \left(\boldsymbol{R}_{\boldsymbol{yx}}\right)^H$.

The parameter $\mathbb{E}\left\{\Omega_l^{(g',g)}(k,m)\right\}$ can be defined with the property in Lemma 1 as

$$\mathbb{E}\left\{\Omega_l^{(g',g)}(k,m)\right\} = \mathbb{E}\left\{\left|\left(\boldsymbol{\phi}_k^{(g',g)}\right)^H\ \mathbf{Q}_l^{(g')}\,\boldsymbol{\phi}_m^{(g',g')}\right|^2\right\} = \mathbb{E}\left\{\left|\mathbf{x}^H\mathbf{A}\mathbf{y}\right|^2\right\} \tag{4.26}$$

where $\mathbf{x} = \boldsymbol{\phi}_k^{(g',g)}$, $\mathbf{y} = \boldsymbol{\phi}_m^{(g',g')}$ and $\mathbf{A} = \mathbf{Q}_l^{(g')}$. Therefore, calculating the covariance matrices $\mathbf{R}_{\mathbf{xx}}$ and $\mathbf{R}_{\mathbf{yy}}$ of the vectors $\mathbf{x}$ and $\mathbf{y}$, together with the matrix $\mathbf{Q}_l^{(g')}$ is enough to calculate the parameter $\mathbb{E}\left\{\Omega_l^{(g',g)}(k,m)\right\}$. The covariance matrix $\mathbf{R}_{\mathbf{xx}}$ of the vector $\mathbf{x}$ can be identified as

$$\mathbf{R}_{\mathbf{xx}} = \mathbb{E}\left\{\boldsymbol{\phi}_k^{(g',g)}\left[\boldsymbol{\phi}_k^{(g',g)}\right]^H\right\} \tag{4.27}$$

where $\boldsymbol{\phi}_k^{(g',g)}$ expression in Eqn. (4.17) can be substituted into Eqn. (4.27) as

$$\mathbf{R}_{\mathbf{xx}} = \left[\mathbf{I}_L \otimes \left[\mathbf{S}^{(g')}\right]^H\right]\left[\sum_{l=0}^{L-1}\mathbf{R}_l^{(g_k)}\right]\left[\mathbf{I}_L \otimes \mathbf{S}^{(g')}\right] \tag{4.28}$$

because the following equation occurs

$$\begin{bmatrix}\mathbf{H}_0^{(g)}(:,k)\\ \mathbf{H}_1^{(g)}(:,k)\\ \vdots\\ \mathbf{H}_{L-1}^{(g)}(:,k)\end{bmatrix}\begin{bmatrix}\mathbf{H}_0^{(g)}(:,k)\\ \mathbf{H}_1^{(g)}(:,k)\\ \vdots\\ \mathbf{H}_{L-1}^{(g)}(:,k)\end{bmatrix}^H = \sum_{l=0}^{L-1}\mathbf{R}_l^{(g_k)} \tag{4.29}$$

A new diagonal elementary matrix $\mathbf{E}_{L,l}$ is defined so that it is an $L \times L$ diagonal elementary matrix such that all diagonal elements other than l^{th} one are zero. Then, $\mathbf{R_{xx}}$ can be written as

$$\mathbf{R_{xx}} = \left[\mathbf{I}_L \otimes \left[\mathbf{S}^{(g')}\right]^H\right] \left[\sum_{l=1}^{L} \mathbf{E}_{L,l} \otimes \mathbf{R}_{l-1}^{(g_k)}\right] \left[\mathbf{I}_L \otimes \mathbf{S}^{(g')}\right] \tag{4.30}$$

and equivalently,

$$\mathbf{R_{xx}} = \sum_{l=1}^{L} \mathbf{E}_{L,l} \otimes \left[\left[\mathbf{S}^{(g')}\right]^H \mathbf{R}_{l-1}^{(g_k)} \mathbf{S}^{(g')}\right] \tag{4.31}$$

$\mathbf{R_{yy}}$ can be found by following the same procedure being done for $\mathbf{R_{xx}}$ as follows

$$\mathbf{R_{yy}} = \mathbb{E}\left\{\boldsymbol{\phi}_m^{(g',g')} \left[\boldsymbol{\phi}_m^{(g',g')}\right]^H\right\} \tag{4.32}$$

and equivalently,

$$\mathbf{R_{yy}} = \sum_{l=1}^{L} \mathbf{E}_{L,l} \otimes \left[\left[\mathbf{S}^{(g')}\right]^H \mathbf{R}_{l-1}^{(g'_m)} \mathbf{S}^{(g')}\right] \tag{4.33}$$

Lastly, the cross covariance matrix $\mathbf{R_{xy}} = \left(\mathbf{R_{yx}}\right)^H$ can be defined as

$$\mathbf{R_{xy}} = \left(\mathbf{R_{yx}}\right)^H = \mathbf{R_{xx}}\ \delta_{g-g'}\delta_{k-m} = \mathbf{R_{yy}}\ \delta_{g-g'}\delta_{k-m} = \mathbf{R_{yx}} \tag{4.34}$$

Finally, after finding the covariance matrices, the parameter $\mathbb{E}\left\{\Omega_l^{(g',g)}(k,m)\right\}$ can be obtained as

$$\mathbb{E}\left\{\Omega_l^{(g',g)}(k,m)\right\} = \mathrm{Tr}\left(\mathbf{A}^H\mathbf{R_{xx}}\mathbf{A}\mathbf{R_{yy}}\right) + \mathrm{Tr}\left(\mathbf{A}\mathbf{R_{yx}}\right)\ \mathrm{Tr}\left(\mathbf{A}^H\mathbf{R_{xy}}\right) \tag{4.35}$$

where this calculation is divided into three parts as

$$\mathbb{E}_1\left\{\Omega_l^{(g',g)}(k,m)\right\} = \mathrm{Tr}\left(\mathbf{A}^H\mathbf{R_{xx}}\mathbf{A}\mathbf{R_{yy}}\right) \tag{4.36}$$

$$\mathbb{E}_2\left\{\Omega_l^{(g',g)}(k,m)\right\} = \mathrm{Tr}\left(\mathbf{A}\mathbf{R}_{\mathbf{yx}}\right) \tag{4.37}$$

$$\mathbb{E}_3\left\{\Omega_l^{(g',g)}(k,m)\right\} = \mathrm{Tr}\left(\mathbf{A}^H\mathbf{R}_{\mathbf{xy}}\right) \tag{4.38}$$

By substituting the covariance matrices into Eqn. (4.36), Eqn. (4.37) and Eqn. (4.38); following matrices are obtained.

$$\mathbb{E}_1\left\{\Omega_l^{(g',g)}(k,m)\right\} = \mathrm{Tr}\left(\left(\mathbf{Q}_l^{(g')}\right)^H\left[\sum_{l_1=1}^{L}\mathbf{E}_{L,l_1}\otimes\mathbf{Z}_{l_1,k}^{(g',g)}\right]\mathbf{Q}_l^{(g')}\left[\sum_{l_2=1}^{L}\mathbf{E}_{L,l_2}\otimes\mathbf{Z}_{l_2,m}^{(g',g')}\right]\right) \tag{4.39}$$

$$\mathbb{E}_2\left\{\Omega_l^{(g',g)}(k,m)\right\} = \mathrm{Tr}\left(\mathbf{Q}_l^{(g')}\left[\sum_{l=1}^{L}\mathbf{E}_{L,l}\otimes\mathbf{Z}_{l,k}^{(g,g)}\right]\delta_{g-g'}\delta_{k-m}\right) \tag{4.40}$$

$$\mathbb{E}_3\left\{\Omega_l^{(g',g)}(k,m)\right\} = \mathrm{Tr}\left(\left(\mathbf{Q}_l^{(g')}\right)^H\left[\sum_{l=1}^{L}\mathbf{E}_{L,l}\otimes\mathbf{Z}_{l,k}^{(g,g)}\right]\delta_{g-g'}\delta_{k-m}\right) \tag{4.41}$$

where $\mathbf{Z}_{l,k}^{(g',g)} = \left(\mathbf{S}^{(g')}\right)^H\mathbf{R}_{l-1}^{(g_k)}\,\mathbf{S}^{(g')}$. Therefore, the parameter $\mathbb{E}\left\{\Omega_l^{(g',g)}(k,m)\right\}$ can be found analytically as

$$\begin{aligned}\mathbb{E}\left\{\Omega_l^{(g',g)}(k,m)\right\} = &\sum_{l_1=1}^{L}\sum_{l_2=1}^{L}\mathrm{Tr}\left\{\left(\mathbf{T}_l^H\mathbf{E}_{L,l_1}\mathbf{T}_l\mathbf{E}_{L,l_2}\right)\otimes\left(\mathbf{Z}_{l_1,k}^{(g',g)}\,\mathbf{Z}_{l_2,m}^{(g',g')}\right)\right\}\\ &+\left[\sum_{l_3=1}^{L}\mathrm{Tr}\left\{\left(\mathbf{T}_l^H\mathbf{E}_{L,l_3}\right)\otimes\mathbf{Z}_{l_3,k}^{(g,g)}\right\}\right]^2\delta_{g-g'}\delta_{k-m}\end{aligned} \tag{4.42}$$

where the term $\mathbb{E}\left\{\Omega_l^{(g',g)}(k,m)\right\}$ can be substituted and utilized to find an analytical expression for the received signal power $\mathbb{E}\left\{\left|r_n^{(g_k)}\right|^2\right\}$ in Eqn. (4.22). Although this term is composed of multiple variable matrices, it is easy to calculate given the indices of the term like the multi-path component (MPC) number index l, the group number index g or the user number index k. Chapter 6 includes the simulation results of

the precoder when CMF type precoder is used and analytical solutions are obtained. Although this digital precoder type gives analytical results without no error coming from the Monte Carlo Simulation, the optimal digital precoder is CMF-SZF type digital precoder since CMF type precoder cannot be used for groups with multi users.

4.1.3 Approximate AIR Calculation

After SINR is calculated analytically or with the help of Monte Carlo Simulation, the user averaged AIR for group g user terminals is defined as

$$\mathrm{AIR}^{(g)} = \frac{1}{K_g} \sum_{k=1}^{K_g} \mathbb{E} \left\{ \log_2 \left(1 + \frac{\left| \beta^{(g_k)} \right|^2}{\left| \xi_n^{(g_k)} \right|^2} \right) \right\} \tag{4.43}$$

where this expression is approximated by using Jensen's inequality as

$$\mathrm{AIR}^{(g)} \approx \frac{1}{K_g} \sum_{k=1}^{K_g} \log_2 \left(1 + \mathbb{E} \left\{ \frac{\left| \beta^{(g_k)} \right|^2}{\left| \xi_n^{(g_k)} \right|^2} \right\} \right) \tag{4.44}$$

where $\mathrm{AIR}^{(g)}$ is further approximated as

$$\mathrm{AIR}^{(g)} \approx \frac{1}{K_g} \sum_{k=1}^{K_g} \log_2 \left(1 + \frac{\mathbb{E} \left\{ \left| \beta^{(g_k)} \right|^2 \right\}}{\mathbb{E} \left\{ \left| \xi_n^{(g_k)} \right|^2 \right\}} \right) \tag{4.45}$$

where SINR expression can be substituted to this approximation as

$$\mathrm{AIR}^{(g)} \approx \frac{1}{K_g} \sum_{k=1}^{K_g} \log_2 \left(1 + \mathrm{SINR}^{(\mathrm{g_k})} \right) \tag{4.46}$$

Thus, if SINR is calculated from the expectations analytically or with Monte Carlo Simulation, AIR is also found with SINR values.

CHAPTER 5

USER GROUPING ALGORITHMS FOR HYBRID BEAMFORMING BASED MASSIVE MIMO SYSTEMS

As mentioned in Chapter 2, once the channel state information reaches the base station and channel covariance matrices of each user terminal are generated, they are optimally distributed to the groups according to a user grouping algorithm before passing through the digital precoder and analog beamformer in order to obtain the best performance results. The user grouping algorithm that is proposed in this chapter partitions the user terminals supported by the base station into multiple groups and each group has its own channel covariance matrix. That is, the user terminals that are distributed to the same group by the user grouping algorithm have the same channel group covariance matrix. This user grouping algorithm is based on the merge and split based algorithm inspired by [25]. However, we design our own performance metric to work with the merge and split type user grouping algorithm, called as AIR metric. As another option, a user grouping algorithm is designed by using only K-means algorithm in order to compare the results of the proposed algorithm with it.

5.1 Algorithms of User Grouping

Two types of user grouping algorithms are investigated throughout this section.

5.1.1 K-Means Algorithm

To obtain a better user grouping distribution than a blind distribution, K-means algorithm is designed as in Algorithm 1.

Algorithm 1 K-means Initialization

1: Choose a random G_0 for the number of groups and select G_0 number of users randomly among K users. Let $\mathbf{U}_g = \mathbf{U}_{k_g}$, where the columns of $\mathbf{U}_{k_g}$ are the M dominant eigenvectors of $\mathbf{R}_{k_g} = \sum_{l=0}^{L} \mathbf{R}_l^{(g_k)}$. M is the number of dominant eigenvalues of $\mathbf{R}_{k_g}$, meaning that the sum of these dominant eigenvalues are greater than 90% of the sum of all eigenvalues of $\mathbf{R}_{k_g}$.

2: For each user k, choose an optimum group g that makes the term $||\mathbf{U}_k\mathbf{U}_k^H - \mathbf{U}_g\mathbf{U}_g^H||_F^2$ minimum among all groups. Put each user in its own group that makes the term minimum.

3: Set $\mathbf{U}_g = \sum_{k=1}^{K_g} \mathbf{R}_{k_g}$.

4: Repeat from step 2 until the user grouping set does not change anymore after several trials.

5.1.2 Merge and Split Based Algorithm with K-Means Initialization and AIR Metric

The merge and split algorithm is widely used in wireless communication systems and game theory [27], [28]. Given the channel covariance matrices of the users to it, this algorithm finds the optimum user grouping that has the maximum total AIR metric among all feasible user grouping options. This metric is based on CMF type digital precoder and joint angle-delay generalized eigen beamformer (JAD-GEB) type analog beamformer. Given a user grouping set, an achivable information rate value is calculated by using CMF type digital precoder with TDMA type multiplexing for intra-group user terminals and JAD-GEB as analog beamformer. This becomes AIR metric of that user grouping set. Let this metric be called as $f(\Upsilon)$ and it changes the user grouping set Υ which is defined as $\Upsilon \triangleq \{\Upsilon_1, \Upsilon_2, ..., \Upsilon_G\}$ where Υ_g is the set of user terminals in group g with cardinality $|\Upsilon_g| = K_g$. Here, K_g and G are to be optimized through user grouping algorithm. The merge and split based algorithm is explained step by step in Algorithm 2. The merge and split based user grouping algorithm finds the optimal user grouping set $\Upsilon_{optimal}$ in finite steps because the metric $f(\Upsilon)$ is a strictly increasing function and it finally reaches to the optimal user grouping set $\Upsilon_{optimal}$ that causes the maximum AIR metric and maximum performance. To obtain

a final maximum AIR metric, a good initial user grouping set should be given to the algorithm as an input. If the initial user grouping is $\Upsilon = \Upsilon_1 = \{1, 2, ..., K\}$ meaning that all user terminals in the system are in the same group or $\Upsilon = \{\{1\}, \{2\}, ..., \{K\}\}$ meaning that there is no user grouping because each user terminal corresponds to a group, then it takes too much time to merge or split the groups to find a final optimum result. Therefore, to give a strong initialization to the algorithm as an input, another user grouping algorithm called K-means initialization can be utilized. It is summarized in Algorithm 1.

Algorithm 2 User Grouping Algorithm Based on Merge and Split Algorithm

1: Give an initial user grouping set to the algorithm manually or take it from the output of K-means initialization.
2: Select two groups randomly. Merge them if the resulting AIR metric $f(\Upsilon_{merged})$ of the new user grouping set is greater than the old metric $f(\Upsilon_{unmerged})$. If it is not greater than the old metric, do not merge them, make the user grouping set remain unchanged.
3: Select a single group randomly. Split the users of this group into two groups if the resulting AIR metric $f(\Upsilon_{splitted})$ of any split combination of the users into two groups is greater than the old metric $f(\Upsilon_{unsplitted})$. If all split combinations are lower than the old metric, do not split it, make the user grouping set remain unchanged.
4: Repeat from step 2 until the user grouping set does not change after some trials.

5.2 AIR Metric Calculation for User Grouping

In order to calculate the AIR metric $f(\Upsilon)$, the achievable information rate $\mathrm{AIR}^{(g_k)}$ for each user terminal can be calculated by ignoring the existence of all intra-group user terminals other than the k^{th} one as

$$\mathrm{AIR}^{(g_k)}_{no-intra} \triangleq \min\{1, \frac{\tau^{(g)}}{K_g}\} \log_2\left(1 + \mathrm{SINR}^{(g_k)}_{no-intra}\right) \tag{5.1}$$

where the parameter $\tau^{(g)} = 1$ for TDMA and $\tau^{(g)} > 1$ for NOMA and $\mathrm{SINR}^{(g_k)}_{no-intra}$

is stated as

$$\mathrm{SINR}_{no-intra}^{(g_k)} = \frac{\mathbb{E}\left\{\left|\beta^{(g_k)}\right|^2\right\}}{\mathbb{E}\left\{\left|\xi_{n,\{no-intra\}}^{(g_k)}\right|^2\right\}} \tag{5.2}$$

where $\mathbb{E}\left\{\left|\beta^{(g_k)}\right|^2\right\}$ and $\mathbb{E}\left\{\left|\xi_{n,\{no-intra\}}^{(g_k)}\right|^2\right\}$ are identified in terms of the parameter $\mathbb{E}\left\{\Omega_l^{(g',g)}(k,m)\right\}$ mentioned in Chapter 4 as follows:

$$\mathbb{E}\left\{\left|\beta^{(g_k)}\right|^2\right\} = c^{(g)}\ \mathbb{E}\left\{\Omega_0^{(g,g)}(k,k)\right\} \tag{5.3}$$

and the expectation $\mathbb{E}\left\{\left|\xi_{n,\{no-intra\}}^{(g_k)}\right|^2\right\}$ can be expressed as

$$\mathbb{E}\left\{\left|\xi_{n,\{no-intra\}}^{(g_k)}\right|^2\right\} = \underbrace{\sum_{\substack{g'=1\\g'\neq g}}^{G} c^{(g')} \sum_{l=-(L-1)}^{L-1} \sum_{m=1}^{K_{g'}} \mathbb{E}\left\{\Omega_l^{(g',g)}(k,m)\right\}}_{Inter-group\ \ Interference} + \underbrace{c^{(g)} \sum_{\substack{l=-(L-1)\\l\neq 0}}^{L-1} \mathbb{E}\left\{\Omega_l^{(g,g)}(k,k)\right\}}_{Inter-Symbol\ \ Interference} + \underbrace{N_0}_{AWGN} \tag{5.4}$$

The signal powers in Eqn. (5.3) and Eqn. (5.4) are able to be calculated analytically, given the analog beamforming matrices $\left\{\mathbf{S}_{JAD-GEB}^{(g)}\right\}_{g=1}^{G}$ for joint angle-delay generalized eigen beamformer (JAD-GEB) and the power scaling factors $c^{(g)}$'s. After $\mathrm{AIR}_{no-intra}^{(g_k)}$ values are calculated, the total achievable information rate AIR_{Total} is the resulting AIR metric and can be mathematically shown as

$$\mathrm{AIR}_{Total} = \sum_{g=1}^{G} \sum_{k=1}^{K_g} \mathrm{AIR}_{no-intra}^{(g_k)} \tag{5.5}$$

The merge and split based algorithm finds the maximum AIR_{Total} value by taking the analog beamforming matrices $\left\{\mathbf{S}_{JAD-GEB}^{(g)}\right\}_{g=1}^{G}$ of the groups for joint angle-delay

generalized eigen beamformer (JAD-GEB), the power scaling factors $c^{(g)}$'s and the given user grouping set Υ whose the AIR metric are wanted to be calculated. It takes them as inputs and decides the resulting user grouping set $\Upsilon_{optimal}$ as

$$\Upsilon_{optimal} = \arg\max_{\{\Upsilon\}} \ \mathrm{AIR}_{Total}\left(\left\{\mathbf{S}_{JAD-GEB}^{(g)}\right\}_{g=1}^{G}, \left\{c^{(g)}\right\}_{g=1}^{G}, \Upsilon\right) \tag{5.6}$$

The resulting optimal user grouping algorithm is utilized in the analog beamformer part of the system. After user terminals are partitioned into the groups optimally through the user grouping algorithm, the channel covariance matrices $\mathbf{R}_l^{(g)}$ of all groups are calculated. With the channel covariance matrices of all groups, the analog beamformer creates the beams for each group. The optimal user grouping algorithm that finds the best user grouping set in the shortest time interval is the merge and split based algorithm with AIR metric by using K-means initialization to give a good initial user grouping set to the algorithm. The simulation results of the comparison of the user grouping algorithms can be found in Chapter 6.

CHAPTER 6

SIMULATION RESULTS AND DISCUSSION

As expressed in the earlier chapters, the performance measurement parameter of this research is the achievable information rate or AIR in short. The performance of the hybrid structure is measured by observing the achievable information rate changes when different parameters of the system are varied. In order to show the simulation results of the study, we should firstly define a scenario that is worked on throughout the thesis.

6.1 Scenario

In order to investigate all cases, the scenario should include all types of the groups like a group having a single user, a group having a single MPC or a group having multi users and more than one MPCs. In the studied scenario, the base station is designed with a uniform linear array (ULA) with $N = 100$ antenna elements. Each user terminal is equipped with a single antenna element. There are $L = 16$ MPC's in the system and the MPCs of each user are sparsely distributed in the angle-delay plane. At BS, there are total of $D = 12$ RF chain components and these RF chains are distributed to each group related to their MPC numbers (L_g) and their user numbers (K_g) told in the inter-group RF chain distribution part of the thesis. In the system, there are $K = 10$ user terminals each with different MPCs as in Table 6.1. From the angle of arrival (AoA) values and the angular spreads of the user terminals, the covariance matrices $\mathbf{R}_l^{(k)}$ of the user terminals are generated. After that, these user terminals should be grouped via a user grouping algorithm to create the beams of each group properly in analog beamformer part. The user grouping algorithm can be

designed as an only K-means algorithm or it can be implemented with only merge and split algorithm that takes a user grouping set manually as an input. To reach the resulting user grouping set that is optimal to obtain the best performance, a hybrid user grouping is proposed. The proposed user grouping structure is that the user grouping algorithm can be designed as the merge and split based algorithm initialized by the K-means algorithm. The output of the K-means algorithm can be used in merge and split algorithm as an initialization. With this way, the merge and split based user grouping algorithm can reach the optimal user grouping much faster with less trials. The proposed user grouping algorithm results in a user grouping set that has four groups ($G = 4$) shown in Table 6.2. The angle-delay plane map of the resulting user grouping distribution by using merge and split based user grouping algorithm can be seen in Figure 6.1. In this map, different edgecolors represent the multi-path components of different groups. As can be observed, the merge and split based user grouping algorithm optimally distributes the user terminals without any angle alignment in inter-group multi-path components. There is no any overlapping MPC between different groups. This is important because if there would be any overlapping MPC, the analog beamformer creates a beam just on the angular sector of the inter-group multi-path components and this situation decreases the performance of the precoder considerably.

As an analytical example, for $30GHz$ systems with $B = 100MHz$ intervals, it can be calculated that ULA $\lambda = 1cm$, $N = 100$ and there is $50cm$ antenna array. If the distance between two scatterers, corresponding to two different MPCs of a given user, is $50m$, then this corresponds to $\tau = \frac{50}{c} = 0.66\mu s$ delay making multi-path component number $L = \lfloor \tau B \rfloor = 16$. That is why the studied scenario has $L = 16$ multi-path components.

Table 6.1: Scenario

User	Active MPC Index	Mean AoA	Angular Spread
1	1	-27	2.5
	7	12.6	2.5
2	2	-23	2
	4	7.7	3
	14	27.2	3
3	2	-23	2
	4	7.9	2.5
	14	27.8	2.5
4	9	-12.3	2
	11	17.7	2.5
5	9	-12.2	3
	11	17.3	2
6	9	-12.1	3
	11	18	3
7	13	-2	2
8	13	-2.7	2
9	13	-2.8	2
10	13	-2.5	2

If the user grouping algorithm can be designed as an only K-means algorithm, because of the existence of the randomness in the K-means algorithm, it finds different user grouping results each time it is run. Therefore, the result of the K-means algorithm is not reliable to be used in the system. However, it can give a good initial user grouping to the merge and split algorithm and that is the reason why the proposed user grouping algorithm includes both of the algorithms. An example user grouping result of the K-means algorithm can be seen in Table 6.3. Also, the resulting angle-delay plane map of the resulting user grouping distribution is demonstrated in Figure 6.2. Different edgecolors represent the multi-path components of different groups. As can be seen from the figure, there are overlapping multi-path components between different groups. This overlapping issue can be observed in MPC-9 and MPC-11.

Table 6.2: Resulting Optimal User Grouping Scenario Found by Proposed User Grouping Algorithm

Group	User	Active MPC Index	Mean AoA	Angular Spread
1	1	1	-27	2.5
		7	12.6	2.5
2	2	2	-23	2
		4	7.7	3
		14	27.2	3
	3	2	-23	2
		4	7.9	2.5
		14	27.8	2.5
3	4	9	-12.3	2
		11	17.7	2.5
	5	9	-12.2	3
		11	17.3	2
	6	9	-12.1	3
		11	18	3
4	7	13	-2	2
	8	13	-2.7	2
	9	13	-2.8	2
	10	13	-2.5	2

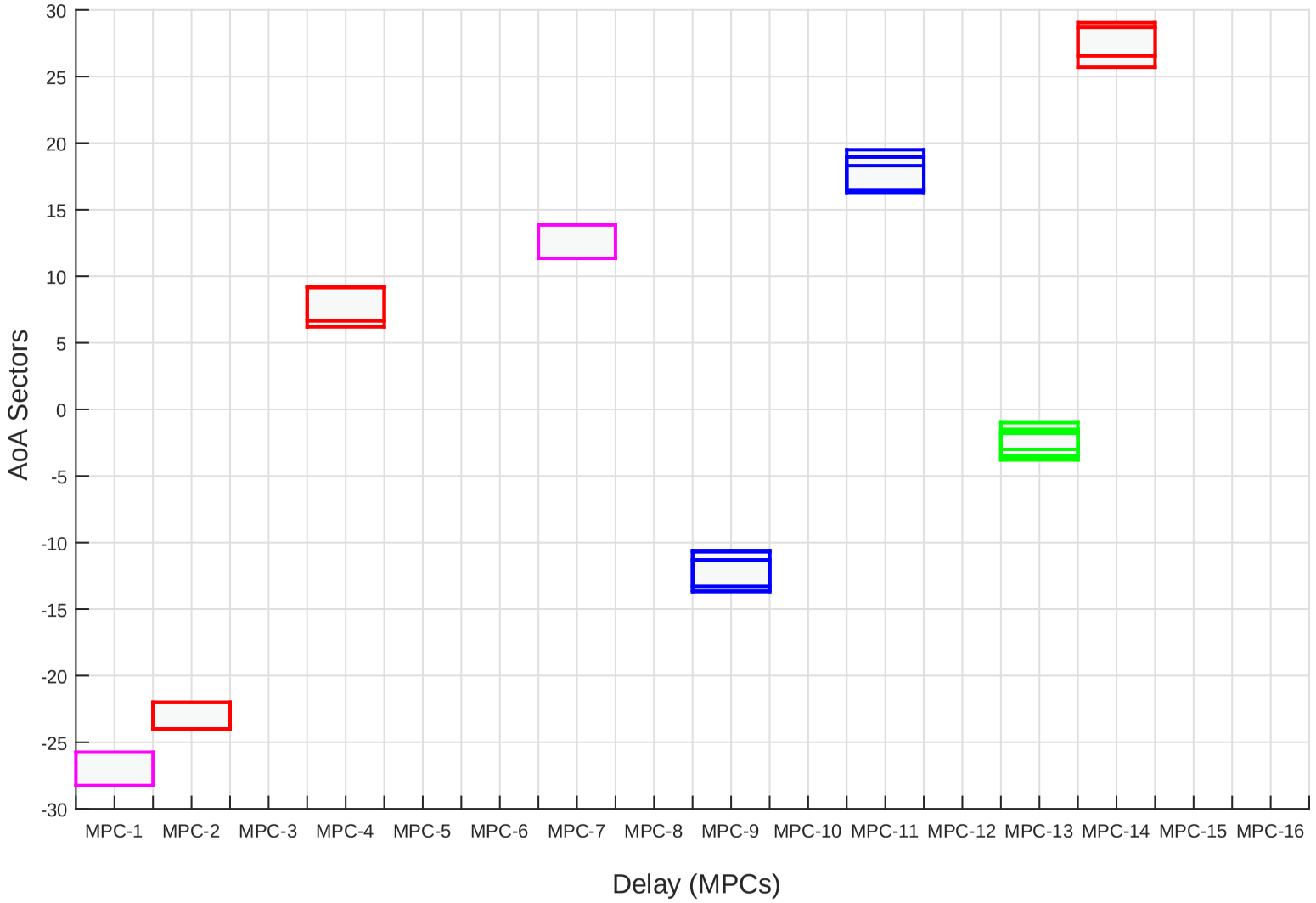

Figure 6.1: Angle-Delay Plane of the Resulting Group Distribution by Using Merge and Split Algorithm

Table 6.3: Resulting User Grouping Scenario Found by Using Only K-Means Algorithm

Group	User	Active MPC Index	Mean AoA	Angular Spread
1	1	1	-27	2.5
		7	12.6	2.5
	7	13	-2	2
	8	13	-2.7	2
	9	13	-2.8	2
	10	13	-2.5	2
2	2	2	-23	2
		4	7.7	3
		14	27.2	3
	3	2	-23	2
		4	7.9	2.5
		14	27.8	2.5
3	4	9	-12.3	2
		11	17.7	2.5
4	5	9	-12.2	3
		11	17.3	2
	6	9	-12.1	3
		11	18	3

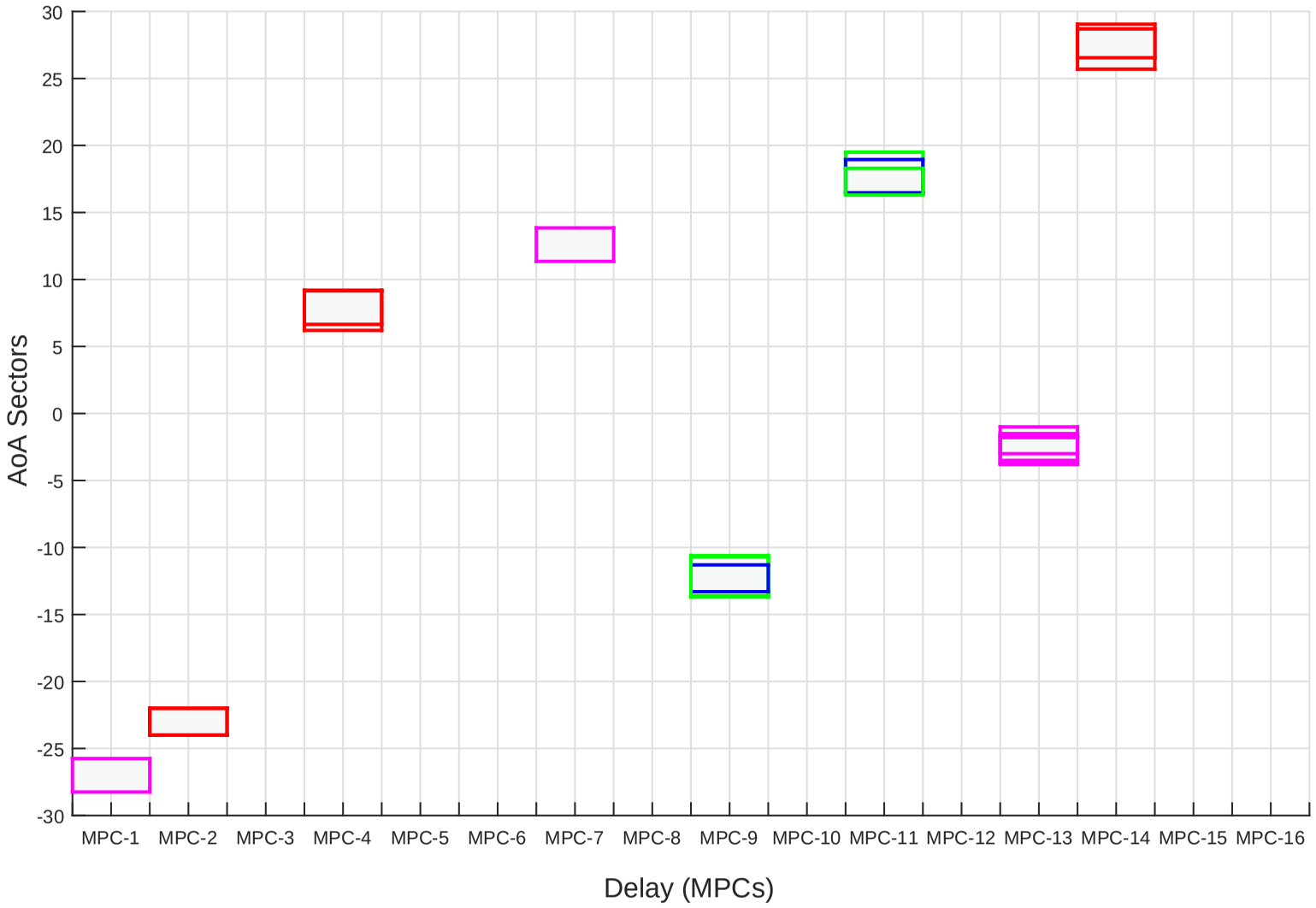

Figure 6.2: Angle-Delay Plane of the Resulting Group Distribution by Using K-Means Algorithm

6.2 Simulation Results

To measure and compare the performance of different designs, different curves are obtained. The subsections show the simulation results by changing several parameters of the system.

6.2.1 AIR vs. Total Transmit Power for Different Analog Beamforming Techniques

First of all, the changes in AIR by changing the total transmit power E_s given to the system at downlink from BS are observed by using different analog beamformer types and different digital precoder types mentioned in the thesis. As a bound to the curves, a nearly full digital ($D = 30$ which is much greater than $D = 12$ in the system) CMF type precoder by assuming zero interference is used. For the bound, angle only eigen beamformer is utilized as the analog beamformer, but this does not affect the bound completely since it is a nearly full digital structure. These figures investigate the performance of the different types of hybrid structures. As the user grouping algorithm, the proposed merge and split based algorithm with K-means initialization together with AIR metric is used. Therefore, before the signals that will be transmitted to the user terminals pass through the hybrid structure, the user grouping algorithm distributes the user terminals to the groups like in Table 6.2.

6.2.1.1 AIR vs. Total Transmit Power for CMF Type Precoder without TDMA

CMF type precoder without TDMA is used as the digital precoder for the plots given in Figures 6.3, 6.4, 6.5 and 6.6. Each figure represents the user averaged AIR of each group by changing the total transmit power given to the system from BS, seperately. The AIR calculation in this type of digital precoder can be analytically operated as stated earlier in Chapter 4. From Figure 6.3, it can be understood that the proposed joint angle-delay generalized eigen beamformer (JAD-GEB) outperforms the best performance compared to the other type of analog beamformers for a group with single user terminal. However, for the multi user groups, CMF type digital precoder

without TDMA does not operate properly for all types of analog beamformers as can be seen from Figures 6.4, 6.5 and 6.6. This means that CMF type digital precoder can be used in single user systems and instead of the Monte Carlo Simulation results, it has reliable analytical results behind it. However, it cannot be used for the systems having groups with multi users.

As the bound, analytical nearly full digital CMF type digital precoder is used by assuming no inter-group and intra-group interference in the system. By this way, for the multi user groups, the bound does not saturate like all the other curves do, because it is assumed that there is no intra-group interference.

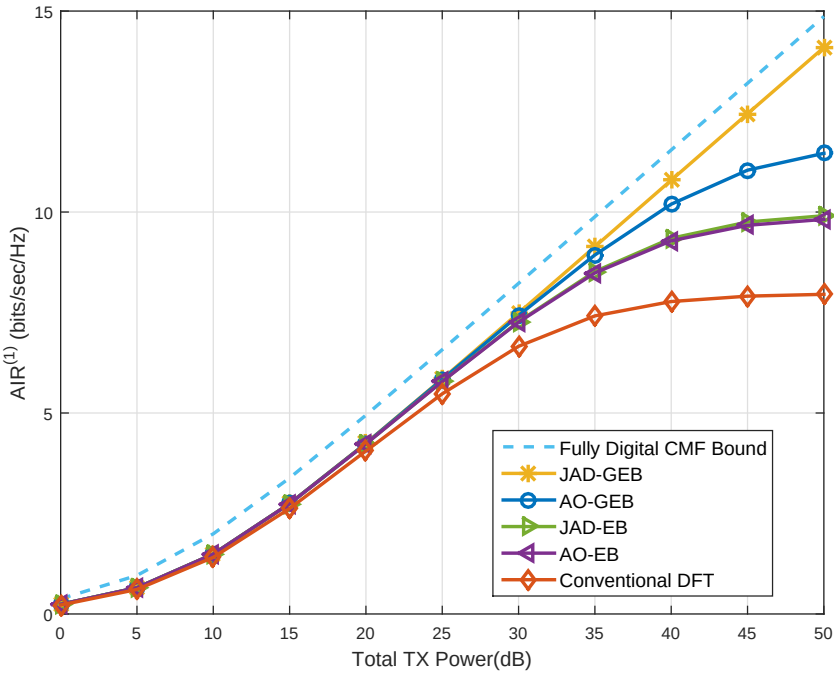

Figure 6.3: AIR of group-1 vs. total transmit power (E_s) with CMF type precoder without TDMA

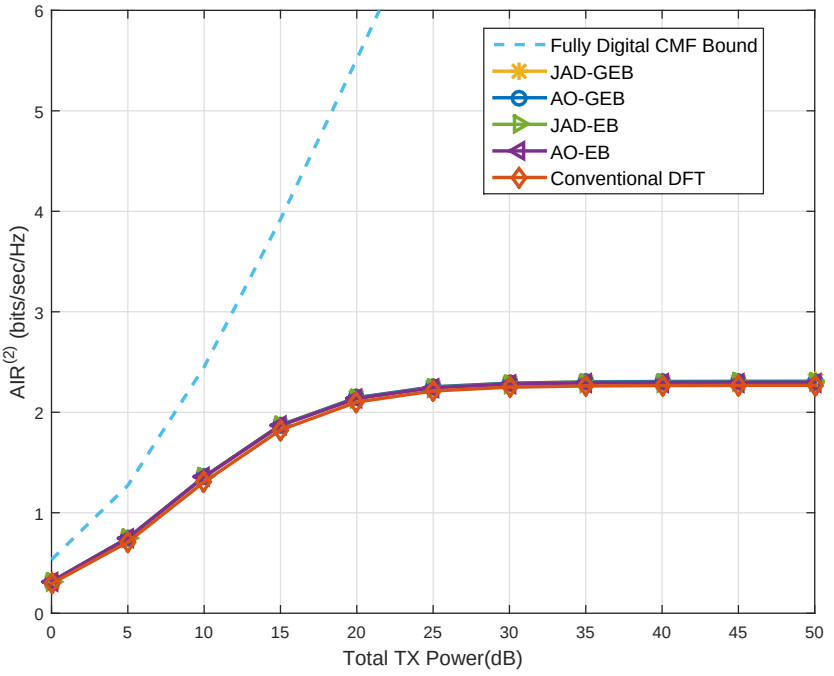

Figure 6.4: AIR of group-2 vs. total transmit power (E_s) with CMF type precoder without TDMA

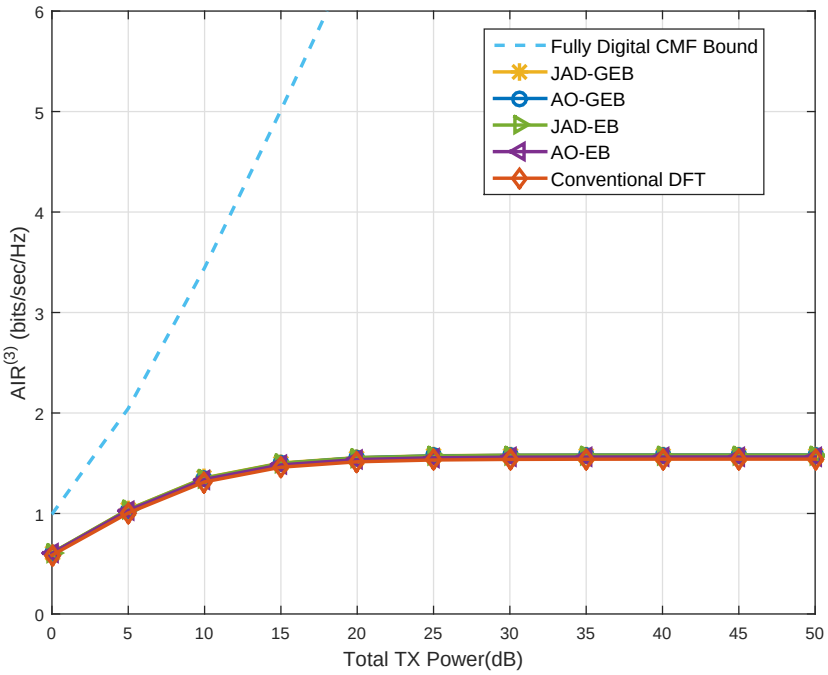

Figure 6.5: AIR of group-3 vs. total transmit power (E_s) with CMF type precoder without TDMA

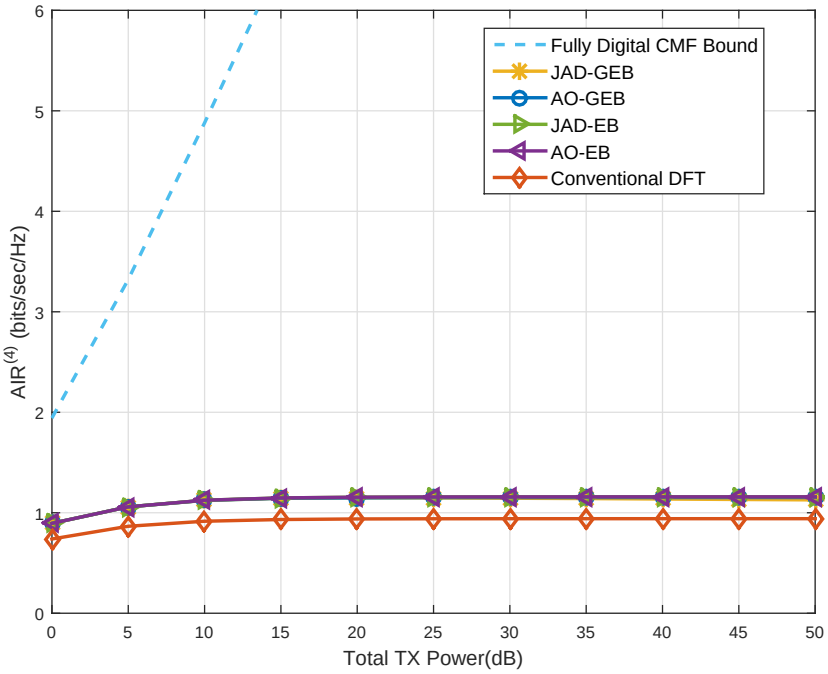

Figure 6.6: AIR of group-4 vs. total transmit power (E_s) with CMF type precoder without TDMA

6.2.1.2 AIR vs. Total Transmit Power for CMF Type Precoder with TDMA

Using TDMA with CMF type precoder can be a solution for the problem with the groups having multi user in CMF type digital precoder as can be seen from Figures 6.8, 6.9 and 6.10 that show AIR values of the groups with multi users while the single user case performance (Figure 6.7) is kept constant with the CMF type digital precoder without TDMA. However, with this type of digital precoder, the user terminals cannot communicate with BS at the same time in the time domain, which affects the channel capacity very badly. In addition to this, the user averaged AIR values is at a very low level compared to the ones of nearly full digital CMF bound with zero interference. In order to compare the performance of this type of digital precoder with a fair bound, a bound is modified as a fully digital CMF type digital precoder with TDMA by assuming no inter-group interference but there is intra-group interference. The results are very promising compared to the CMF type precoder without TDMA. This precoder works properly in both single user and multi user systems. However, because TDMA is adapted to the precoder, it provides lower performance when the number of user terminals in a group increases. In addition to this drawback, the user terminals cannot communicate with BS at the same time domain, which makes this digital precoder useless for current systems with giant number of user terminals.

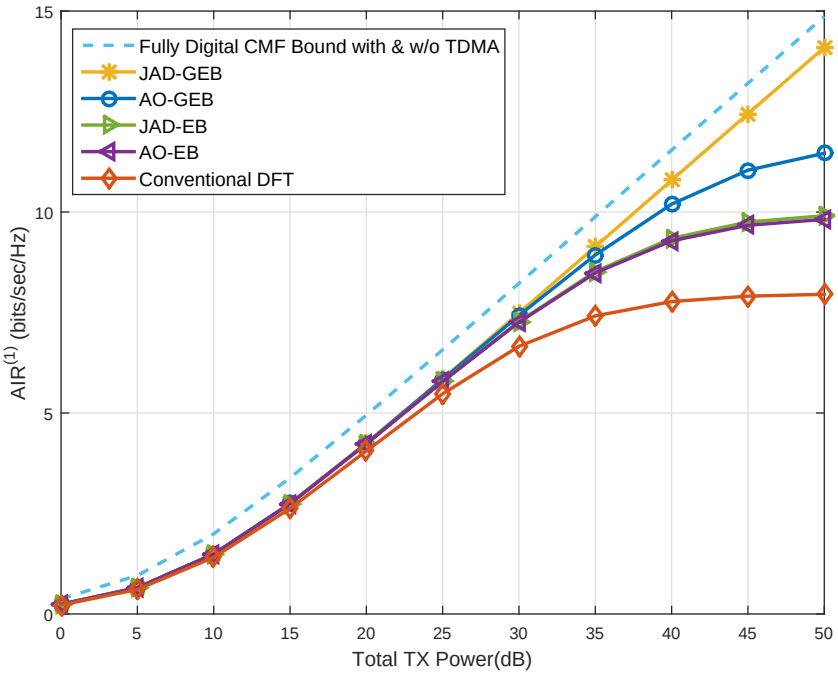

Figure 6.7: AIR of group-1 vs. total transmit power (E_s) with CMF type precoder with TDMA

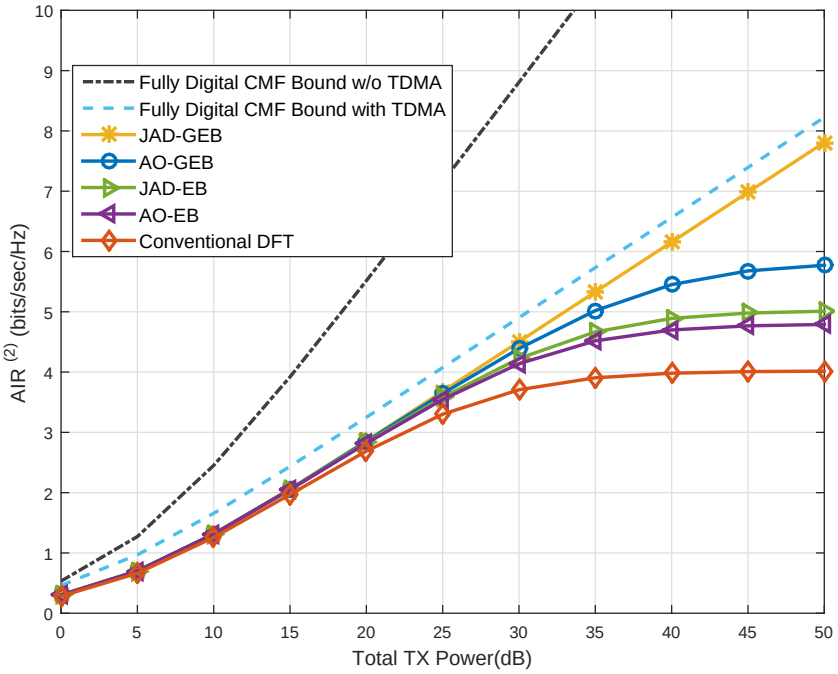

Figure 6.8: AIR of group-2 vs. total transmit power (E_s) with CMF type precoder with TDMA

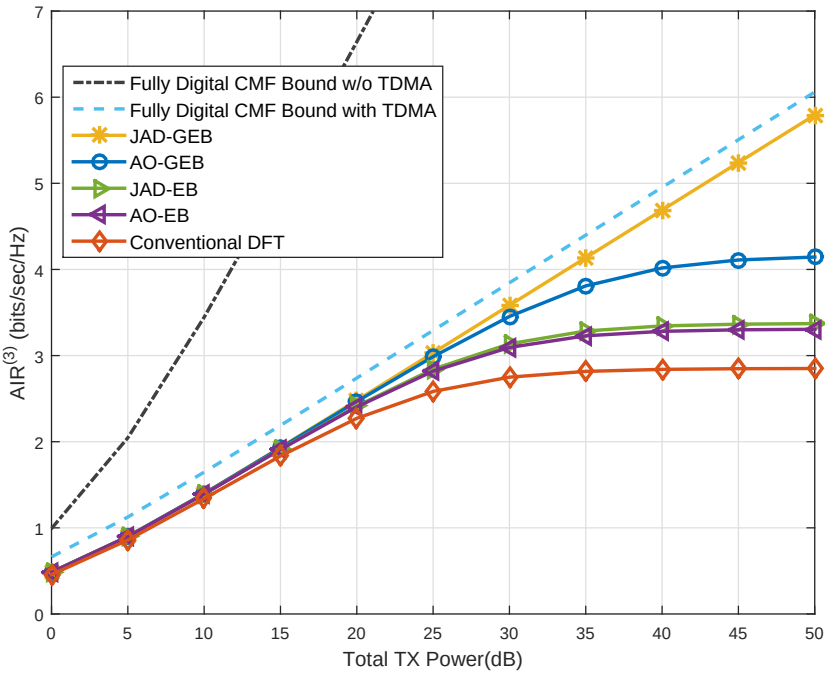

Figure 6.9: AIR of group-3 vs. total transmit power (E_s) with CMF type precoder with TDMA

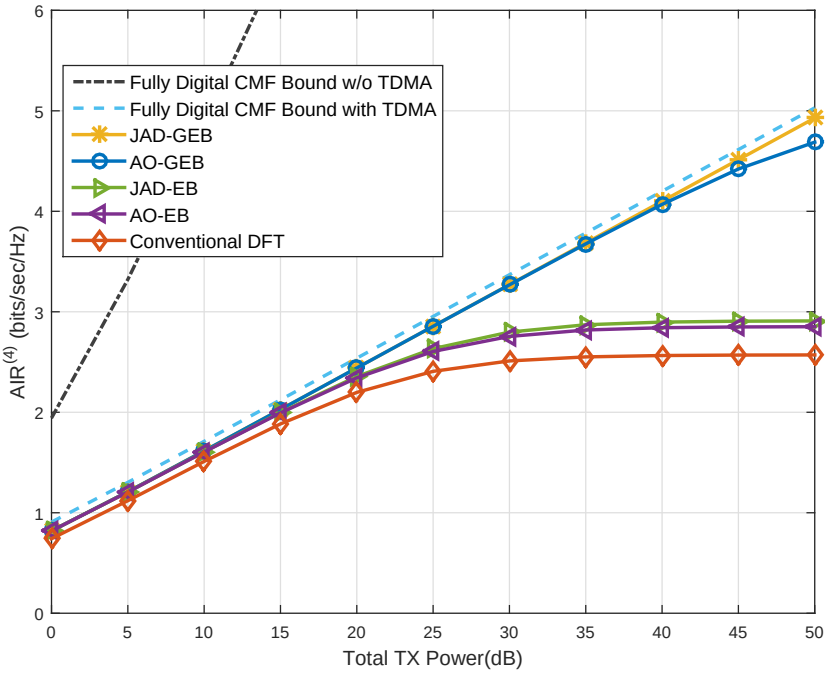

Figure 6.10: AIR of group-4 vs. total transmit power (E_s) with CMF type precoder with TDMA

6.2.1.3 AIR vs. Total Transmit Power for CMF-SZF Type Precoder

Among the three types of digital precoder options, designing CMF-SZF type precoder is the best way to obtain the best performance from the hybrid precoder. As it is demonstrated in Figures 6.11, 6.12 and 6.13, the optimal analog beamformer type which has the closest curve to the bound is the proposed joint angle-delay generalized eigen beamformer (JAD-GEB). In Figure 6.14, because the user terminals in the 4^{th} group have single multi-path component, the proposed joint angle-delay generalized eigen beamformer (JAD-GEB) and the angle only generalized eigen beamformer (AO-GEB) perform exactly the same. For the groups with single MPC, there is no difference between using angle only domain or the joint angle-delay domain. The reason of this is that the positive property of joint angle-delay domain upon the angle only domain cannot be utilized since there is only one MPC in the group. The bound is the analytical nearly digital CMF type digital precoder by assuming zero inter-group and intra-group interference. This digital precoder type is very promising among the other digital precoder types for the groups with multi users. It also provide sufficient performance for the groups with single user. However, it is more convenient to use CMF type digital precoder for the groups with single user because the performance loss of the CMF type digital precoder is less than the performance of CMF-SZF type digital precoder. As another drawback of CMF-SZF type digital precoder, it is not based on an analytical calculation, it can be found with only Monte Carlo Simulation, which makes it less reliable compared to the analytical digital precoder options if there is no enough Monte Carlo sample. If the sample is enough, then, the most optimal digital precoder option is CMF-SZF type digital precoder.

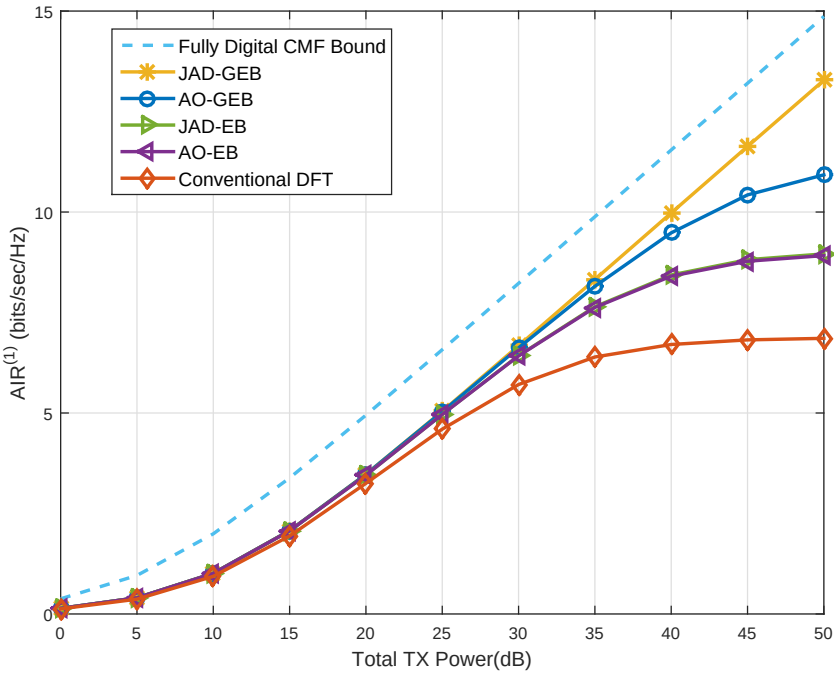

Figure 6.11: AIR of group-1 vs. total transmit power (E_s) with CMF-SZF type precoder

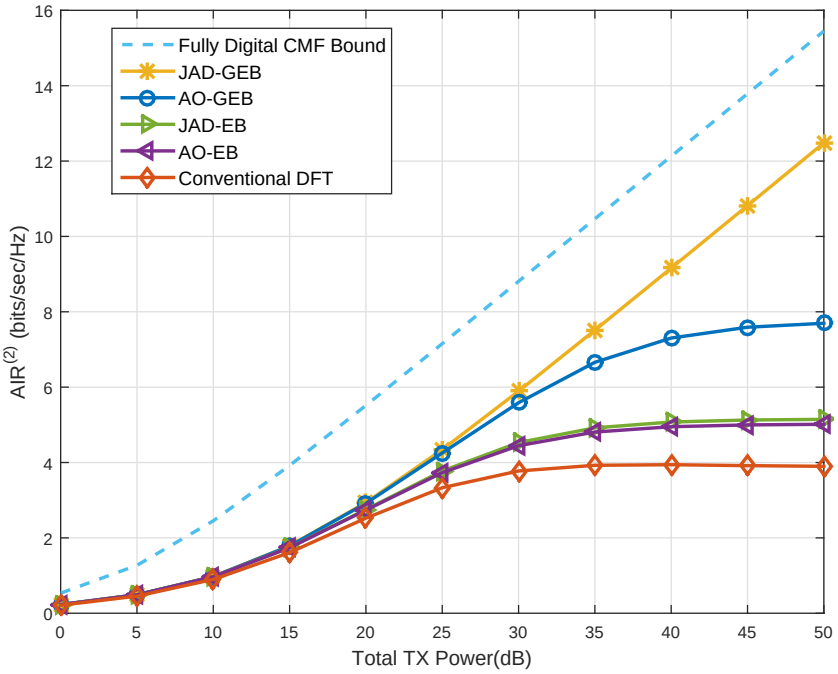

Figure 6.12: AIR of group-2 vs. total transmit power (E_s) with CMF-SZF type precoder

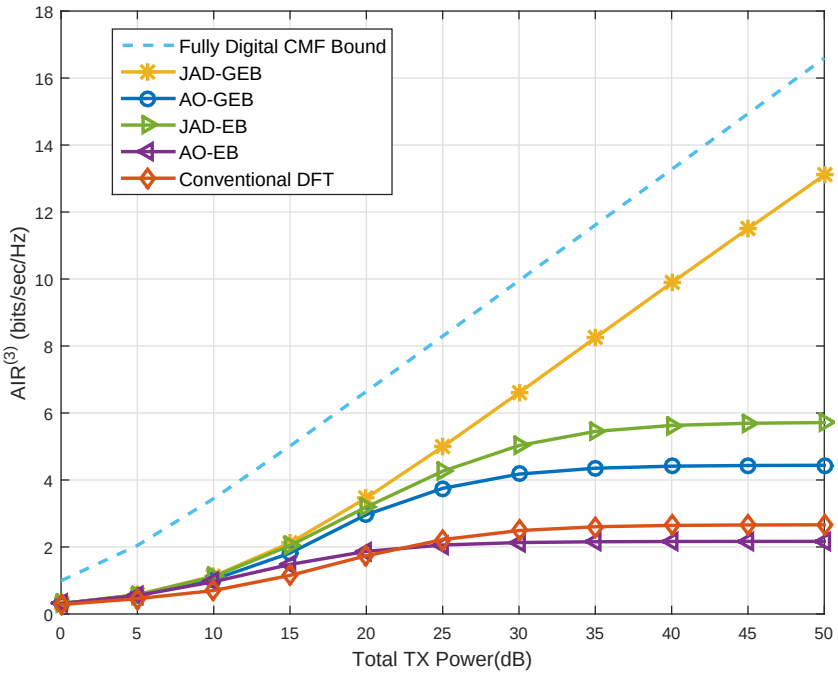

Figure 6.13: AIR of group-3 vs. total transmit power (E_s) with CMF-SZF type precoder

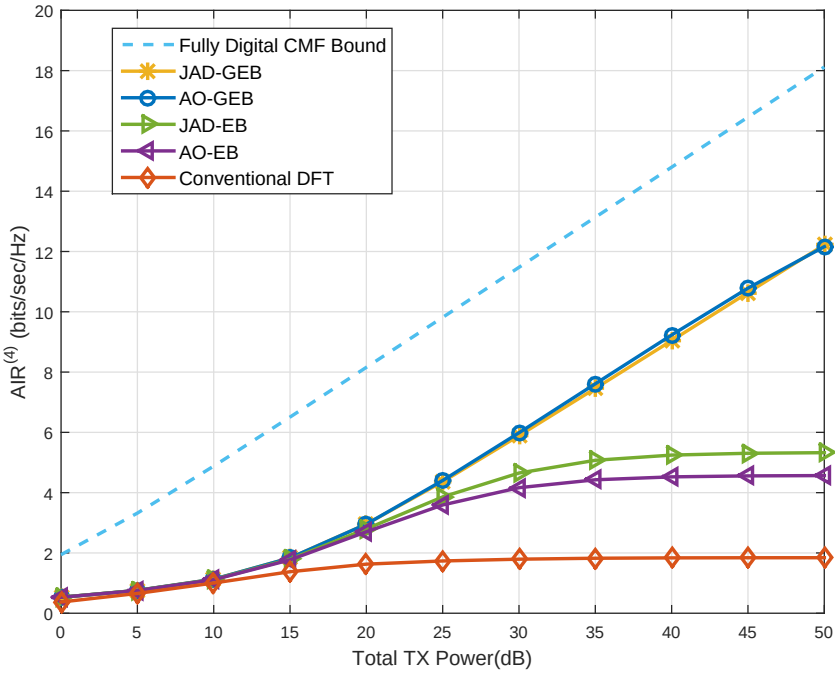

Figure 6.14: AIR of group-4 vs. total transmit power (E_s) with CMF-SZF type precoder

6.2.2 AIR vs. Transmit Power of Interfering Groups for Fixed Desired Group Power for Different Analog Beamforming Techniques

In addition to the investigation of the effect of the total transmit power on the achievable information rate (AIR) of the groups, transmit power of all groups except the desired group can be varied to observe AIR changes of the desired group while the transmit power of the desired group is kept constant. By this way, the effect of the inter-group interference on the AIR of desired group can be observed and different analog beamformers can be compared to each other according to their the inter-group interference suppressing capabilities.

6.2.2.1 AIR vs. Transmit Power of Interfering Groups for Fixed Desired Group Power for CMF Type Precoder without TDMA

As the desired group, 1^{st} group is chosen. Because this group has single user terminal, it is possible to use an analytic digital precoder that is CMF type precoder without TDMA since it works properly for the groups having single user. The transmit power for the desired 1^{st} group is kept constant at $30dB$. According to the simulation results given in Figure 6.15, the proposed joint angle-delay generalized eigen beamformer (JAD-GEB) is flat if the transmit power of the other groups other than the desired one is increased. That is, it is not affected from the inter-group interference. This is because the inter-group interference suppression can be done by using the generalized eigenbeams for beam creation in JAD-GEB. In addition to JAD-GEB, angle only generalized eigen beamformer (AO-GEB) performs almost the same with JAD-GEB. This means that using the generalized eigenbeams in the analog beamformer suppresses the inter-group interference in the system for the groups with single user terminal. The reason that JAD-GEB and AO-GEB operate almost the same is that the transmit power of the desired group is not changed and it is kept at a moderate level ($30dB$). If this level is increased, JAD-GEB starts to operate better compared to AO-GEB. Except these two generalized type analog beamformers, the other three analog beamformer types are affected from the inter-group interference very badly since they do not suppress the multi-path components coming from the inter-group user terminals in their beams.

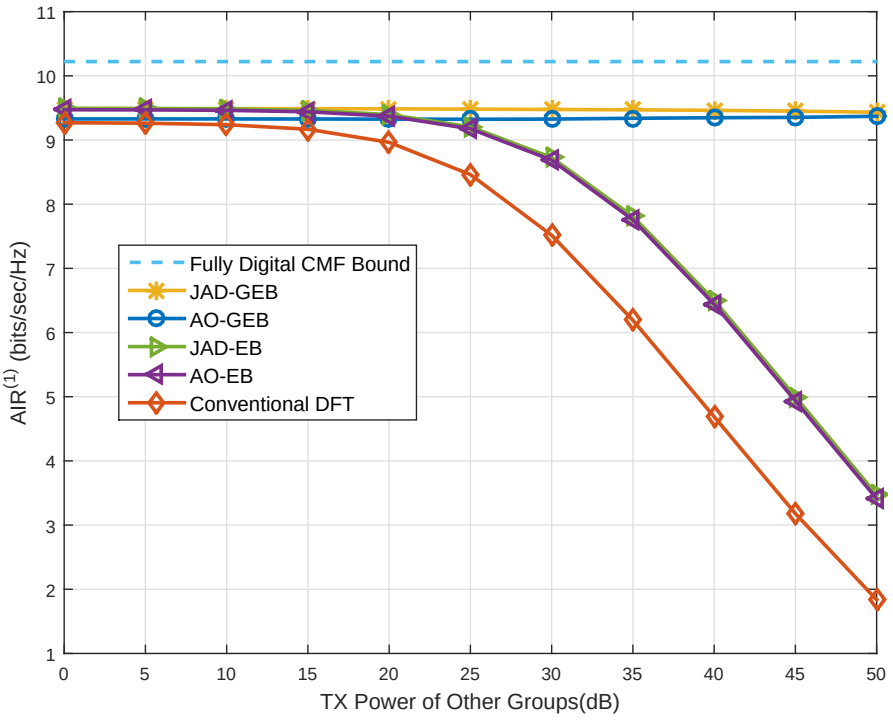

Figure 6.15: AIR of group-1 vs. transmit power of the groups other than the desired group ($E_s^{(g)}$) with CMF type precoder without TDMA

6.2.2.2 AIR vs. Transmit Power of Interfering Groups for Fixed Desired Group Power for CMF-SZF Type Precoder

In addition to the investigation of the single user case, it is also important to observe the inter-group interference suppression capabilities of the analog beamformers when the desired group has more than one user terminal, i.e. multi user case. As the desired group, the 2^{nd} group is chosen. The transmit power for the desired 2^{nd} group is kept constant at $30dB$ while the transmit powers of the other groups other than the desired one vary from $0dB$ to $50dB$. As can be seen from Figure 6.16, the proposed JAD-GEB operates the best and it is not affected by the inter-group interference increase. Compared to the single user case in Figure 6.15, there is some extra loss between the bound and JAD-GEB because of the digital precoder type that is used. As the digital precoer, Channel Matched Filter-Spatial Zero Forcing (CMF-SZF) type precoder is utilized since the other analytical type digital precoders cannot be used because of having multi user system for this simulation.

One of the striking point in Figure 6.16 is that joint angle-delay eigen beamformer (JAD-EB) performance is better than angle only generalized eigen beamformer (AO-GEB) at low levels of transmit powers of the other groups. The reason of this is that there is no need to use generalized eigenbeams to suppress the inter-group interference at low level transmit power since the inter-group interference is very low at these points. For this purpose, using joint angle delay domain in analog beamformer outweighs using the generalized eigenbeams in analog beamformer at low transmit power levels or low inter-group interference. After the inter-group interference increases, AO-GEB performs better than JAD-EB as expected since generalized eigenbeams suppresses the inter-group interference and inter-group interference becomes important when the transmit powers of the other groups increase.

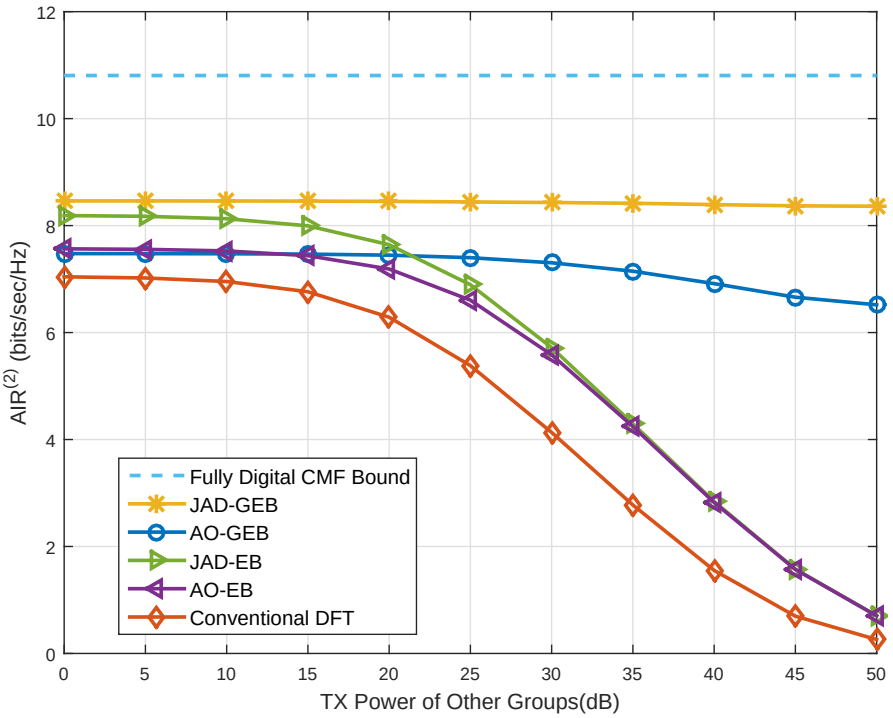

Figure 6.16: AIR of group-2 vs. transmit power of the groups other than the desired group ($E_s^{(g)}$) with CMF-SZF type precoder

6.2.3 Comparison of Different Digital Precoders for JAD-GEB Type Analog Beamformer

After the observation of how different types of analog beamformers and digital precoders operate together are compared in the previous sections with the plots, the comparison of the performances of the digital precoders can be demonstrated in the same figure by using only proposed joint angle-delay generalized eigen beamformer (JAD-GEB) as the analog beamformer of the structure. As the bound, analytical fully digital CMF type precoder with zero interference (no inter-group and intra-group interference) is utilized together with AO-EB as the analog beamformer. For the single user case (Figure 6.17), CMF type precoder without TDMA and with TDMA perform exactly the same as expected. The performance difference between these two digital precoder types appears in the multi user cases (Figures 6.18, 6.19 and 6.20). CMF type precoder with TDMA provides less performance and starts to move away from the bound as the number of user terminals in the group is increased. However, compared to the CMF type digital precoder without TDMA, the one with TDMA performs better for the multi user systems. Also, CMF type precoders with and without TDMA perform better than Channel Matched Filter-Spatial Zero Forcing (CMF-SZF) type precoder for the single user case while CMF-SZF type precoder preponderates over the CMF type precoders with and without TDMA for the multi user case. Generally, the proposed CMF-SZF type digital precoder performs the best and it is nearly optimal for the digital precoder of the system.

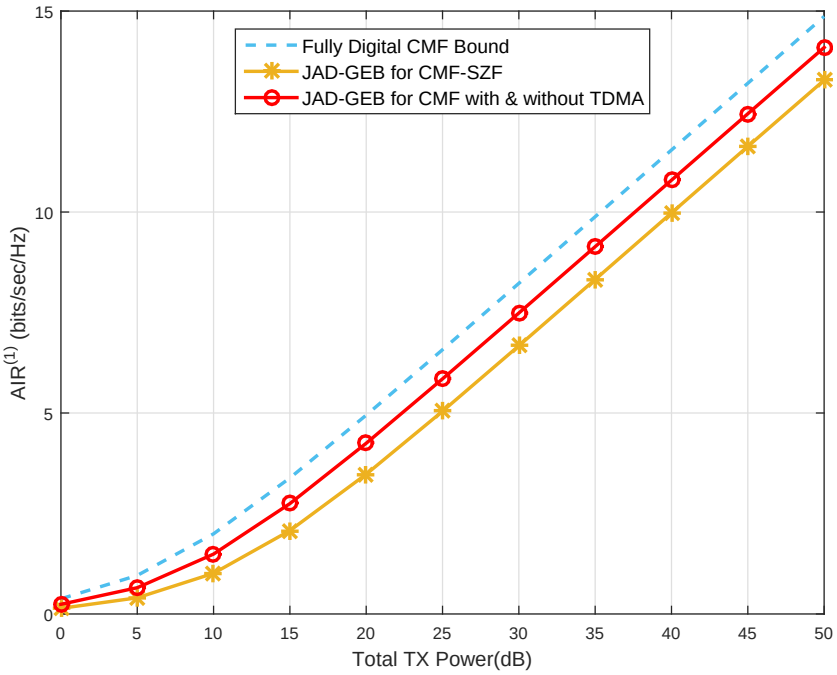

Figure 6.17: AIR of group-1 vs. total transmit power (E_s) with JAD-GEB comparison of all digital precoder types

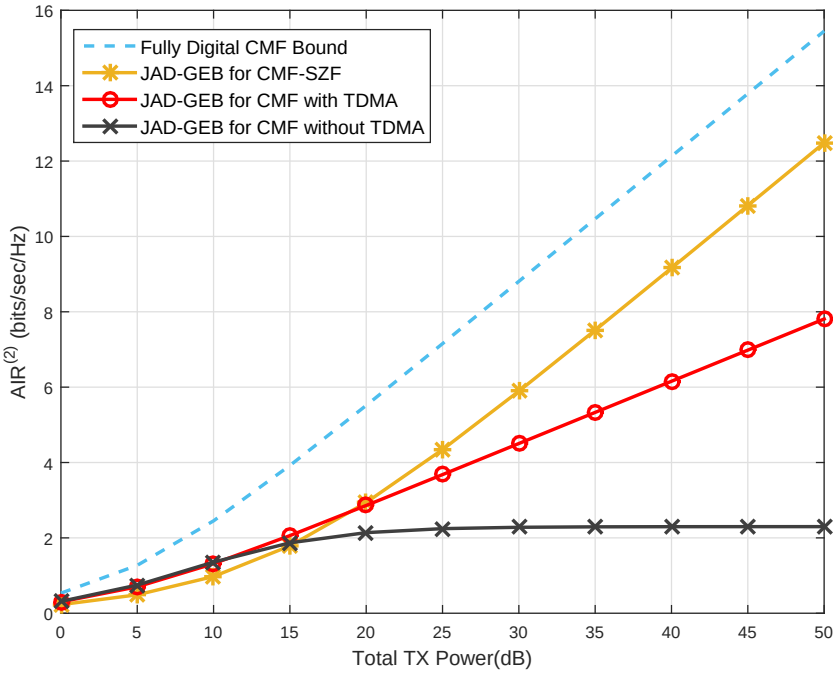

Figure 6.18: AIR of group-2 vs. total transmit power (E_s) with JAD-GEB comparison of all digital precoder types

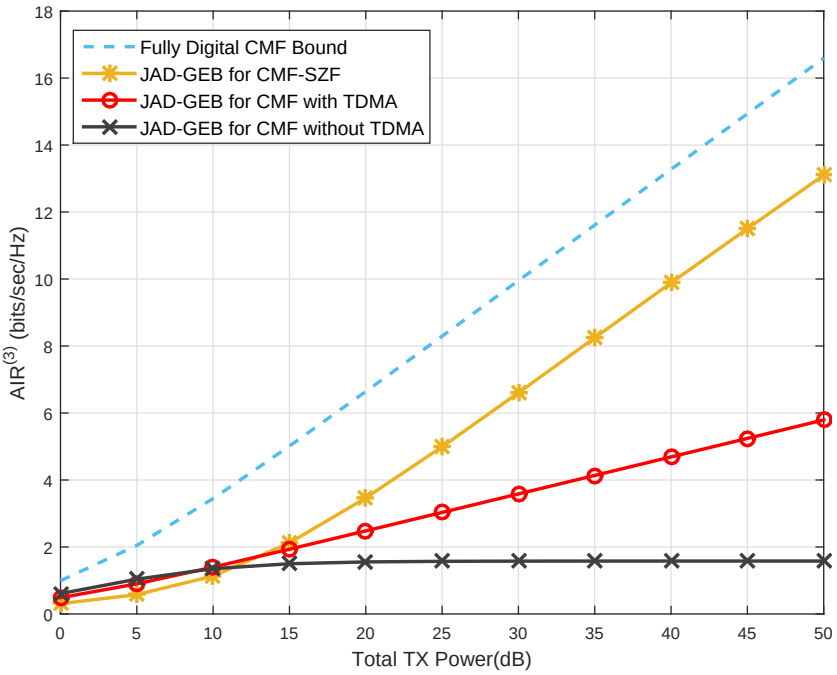

Figure 6.19: AIR of group-3 vs. total transmit power (E_s) with JAD-GEB comparison of all digital precoder types

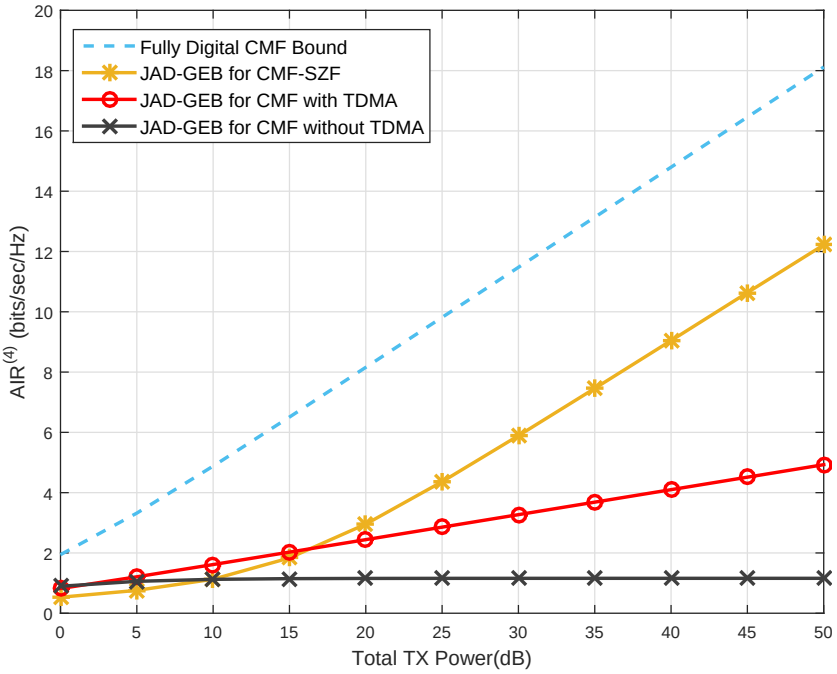

Figure 6.20: AIR of group-4 vs. total transmit power (E_s) with JAD-GEB comparison of all digital precoder types

6.2.4 Comparison of User Grouping Algorithms in terms of Total AIR

With the digital precoder comparison and the analog beamformer comparison, the user grouping algorithm techniques should also be compared to each other. For this purpose, the total achievable information rate AIR_{TOTAL} of the entire channel is the observable parameter and it can be calculated as

$$\mathrm{AIR}_{TOTAL} = \sum_{g=1}^{G} K_g \, \mathrm{AIR}^{(g)} \tag{6.1}$$

The total achievable information rate AIR_{TOTAL} of the entire channel changes are investigated by using different types of user grouping algorithms in the following subsections.

6.2.4.1 Comparison of User Grouping Algorithms in terms of Total AIR for CMF Type Precoder without TDMA

The AIR performance of the CMF type precoder without TDMA in the multi user case is very low whatever the analog beamformer is, as can be seen in Figures 6.4, 6.5 and 6.6. For this reason, using merge and split algorithm or K-means algorithm do not make any difference as it is demonstrated in Figure 6.21. They are far from the analytical nearly full digital CMF type digital precoder bound with zero interference.

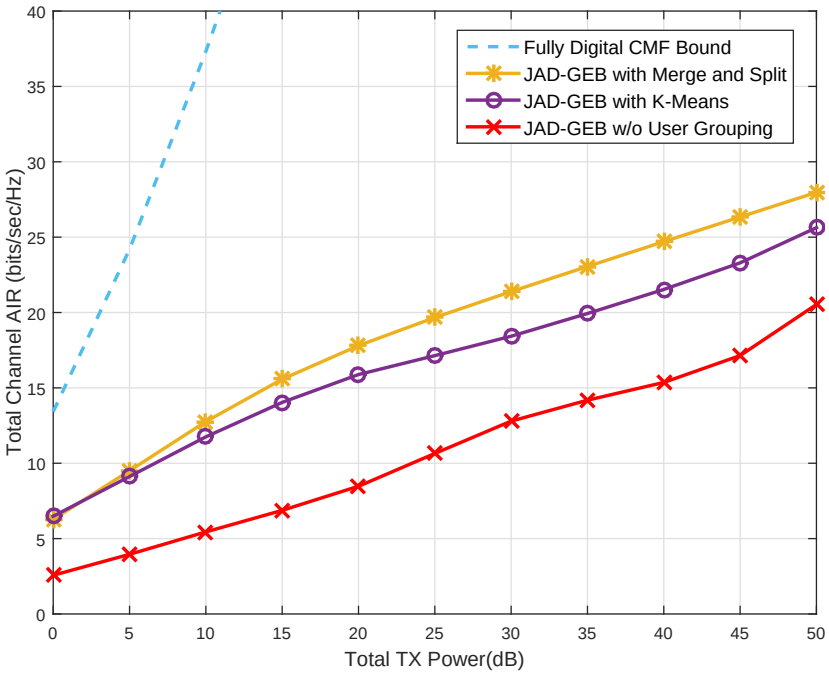

Figure 6.21: Total Channel AIR vs. total transmit power (E_s) for different user grouping algorithm comparison with CMF type precoder without TDMA

6.2.4.2 Comparison of User Grouping Algorithms in terms of Total AIR for CMF Type Precoder with TDMA

If the CMF type precoder with TDMA is chosen as the digital precoder, the multi user operability problem of the CMF type precoder without TDMA can be solved. However, the performance of the digital precoder is still not enough to compare the user grouping algorithm usage results because the performance starts to fall when the number of user terminals in a group increases. Despite the digital precoder problems, merge and split algorithm starts to make a difference as shown in Figure 6.22.

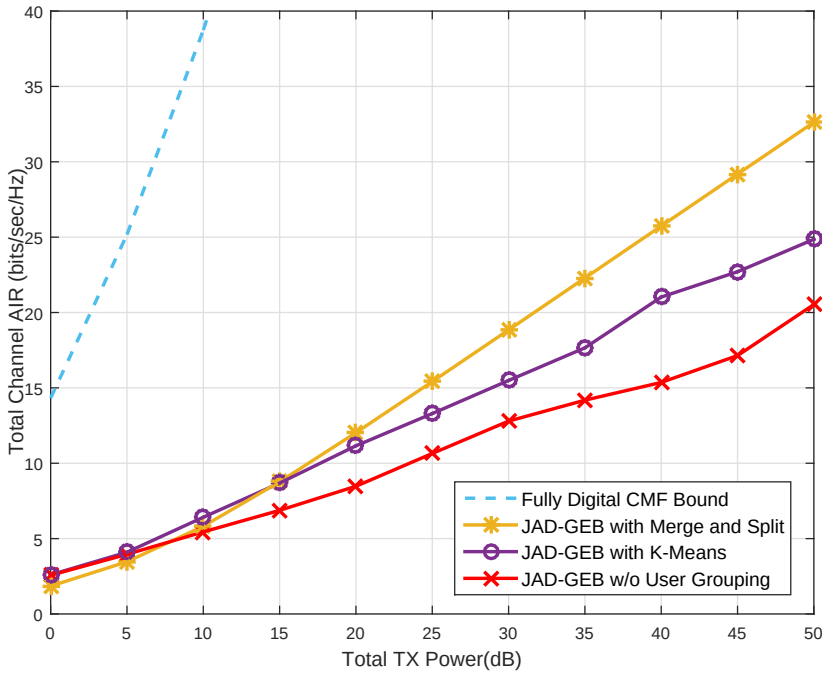

Figure 6.22: Total Channel AIR vs. total transmit power (E_s) for different user grouping algorithm comparison with CMF type precoder with TDMA

6.2.4.3 Comparison of User Grouping Algorithms in terms of Total AIR for CMF-SZF Type Precoder

The merge and split algorithm fully shows its performance with Channel Matched Filter-Spatial Zero Forcing (CMF-SZF) type precoder since this digital precoder works close to the analytical nearly full digital CMF bound with zero interference in all group types (single user or multi user). Figure 6.23 shows that merge and split is by far the optimal user grouping algorithm among the others like K-means or no user grouping. K-means algorithm finds an average user grouping result compared to the case where no user grouping is used.

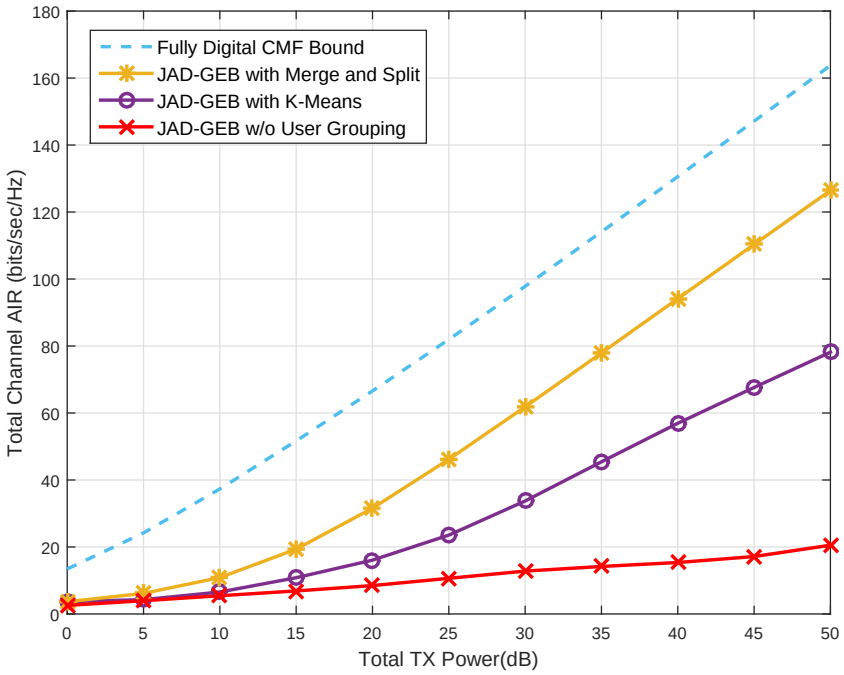

Figure 6.23: Total Channel AIR vs. total transmit power (E_s) for different user grouping algorithm comparison with CMF-SZF type precoder

6.2.5 Beampatterns of Different Analog Beamformers for User Grouping Algorithms

Beampatterns are created in the analog beamformer by using the analog beamforming matrices $\mathbf{S}^{(g)}$ for each group. A beampattern shows how the beams created by the analog beamformer act on the angular sectors shaded from BS and the beampattern of the desired group lightens its multi-path components (MPCs). In addition to lightening, analog beamformers that use the generalized eigenbeams also suppress the inter-group multi-path components coming from the undesired groups. From Figure 6.24 to Figure 6.27, the beampatterns of all analog beamformer types are demonstrated by using K-means algorithm and this algorithm finds a grouping scenario given in Table 6.3. Because group 1 and group 2 of the scenario that K-means algorithm creates do not have any inter-group interference at their own multi-path component indices. This is the reason that the beampatterns for group 1 and group 2 do not have any awkward movement in the beampattern curves (Figures 6.24 and 6.25). However, because the multi-path components of group 3 and group 4 overlap, the inter-group interference increases right at the points where the desired multi-path components exist. This is the reason why a fluctuation occurs in Figures 6.26 and 6.27. Unlike the K-means and its user grouping result, the proposed merge and split algorithm with AIR metric finds an optimal user grouping set distributing each user terminal to groups so that no overlapping multi-path component exists in different groups in the system. The beampatterns of the scenario that merge and split based user grouping algorithm finds can be seen from Figure 6.28 to Figure 6.31. Because the generalized eigen beamformers (JAD-GEB and AO-GEB) suppress the inter-group interferences coming from different groups, their performance becomes better compared to the other analog beamformer types if the transmit power given to the undesired groups is increased. They suppress the undesired multi-path components about $80dB$.

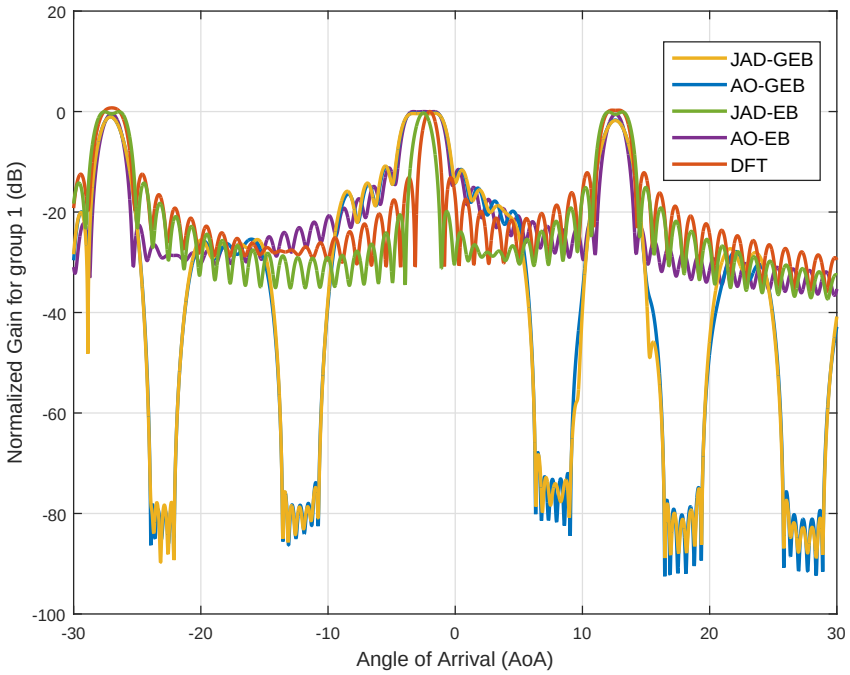

Figure 6.24: Beampatterns of all analog beamformer types in group 1 by using K-Means Algorithm Only

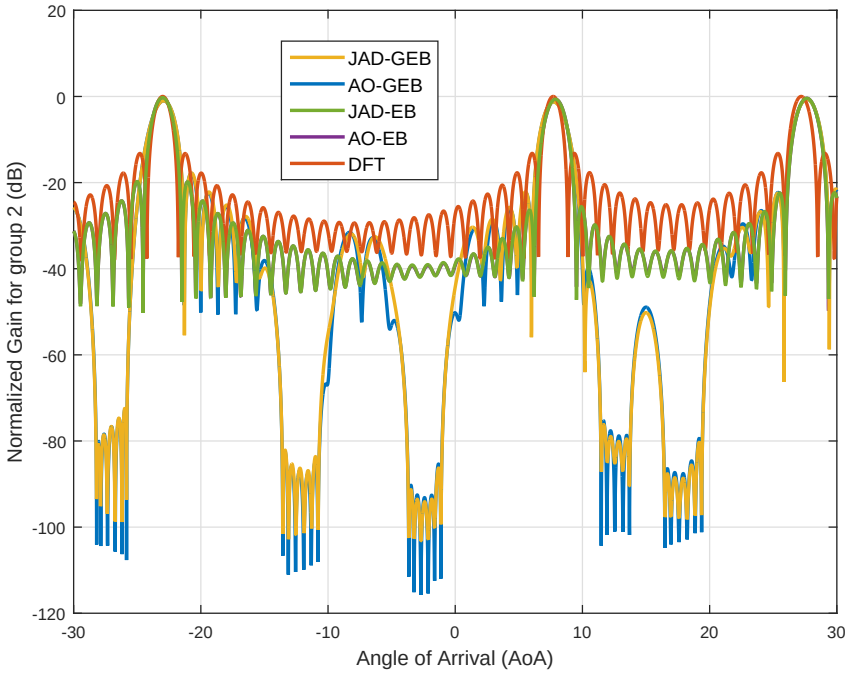

Figure 6.25: Beampatterns of all analog beamformer types in group 2 by using K-Means Algorithm Only

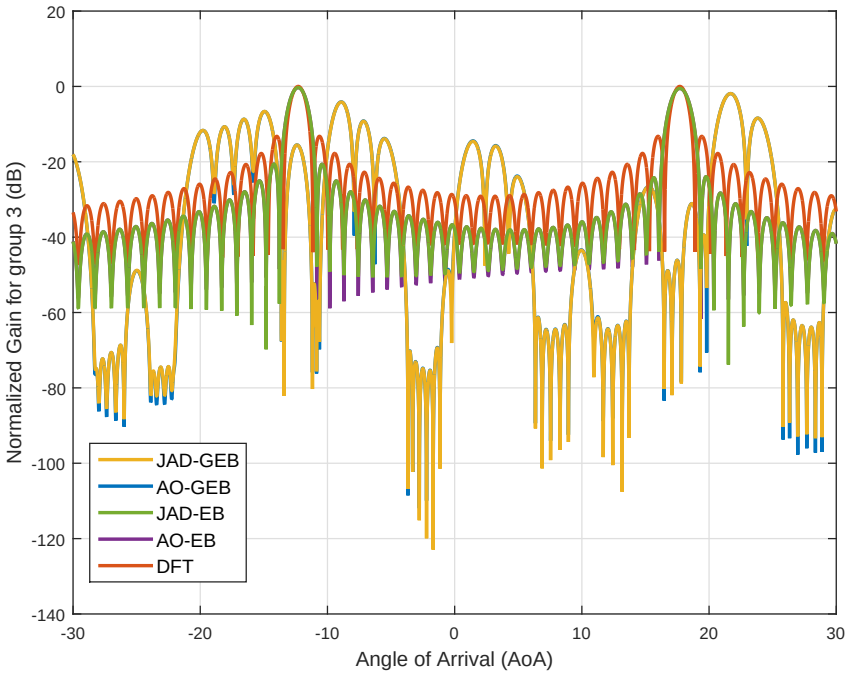

Figure 6.26: Beampatterns of all analog beamformer types in group 3 by using K-Means Algorithm Only

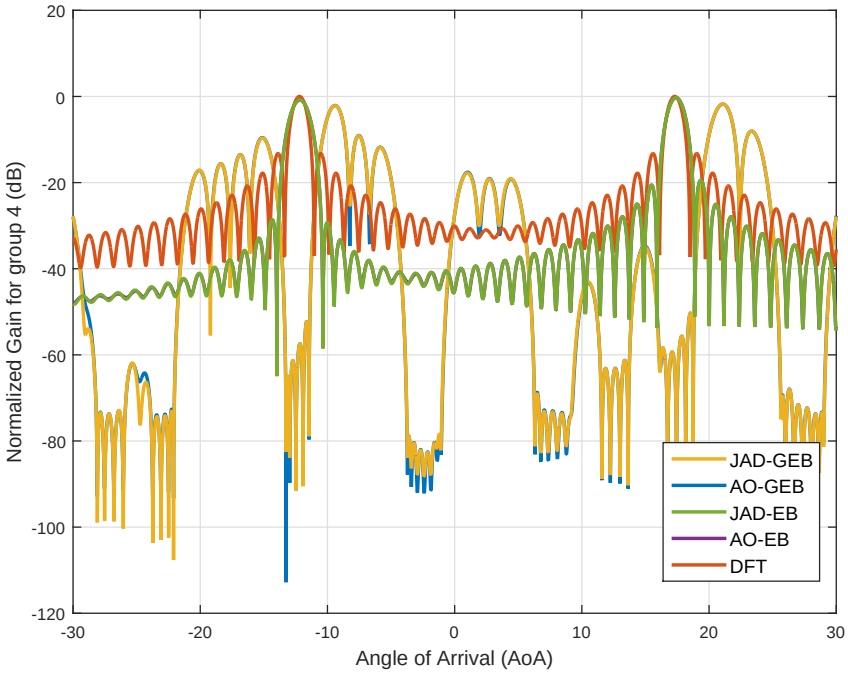

Figure 6.27: Beampatterns of all analog beamformer types in group 4 by using K-Means Algorithm Only

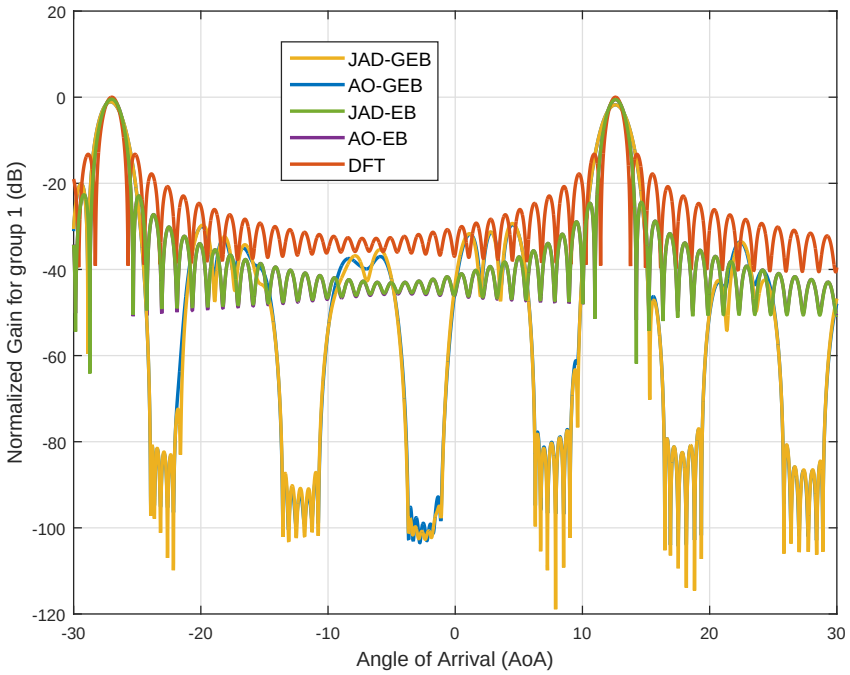

Figure 6.28: Beampatterns of all analog beamformer types in group 1 by using merge and split algorithm

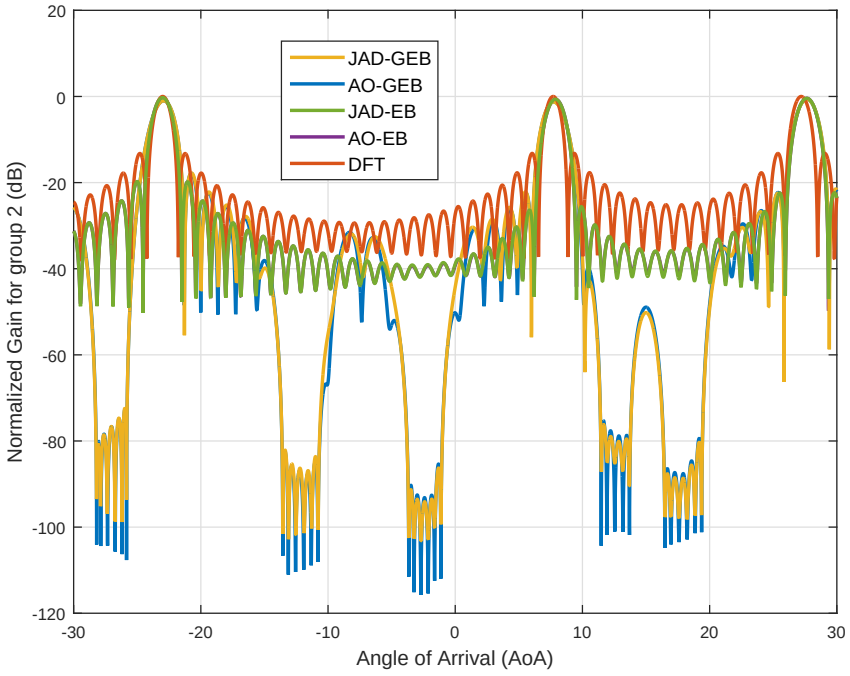

Figure 6.29: Beampatterns of all analog beamformer types in group 2 by using merge and split algorithm

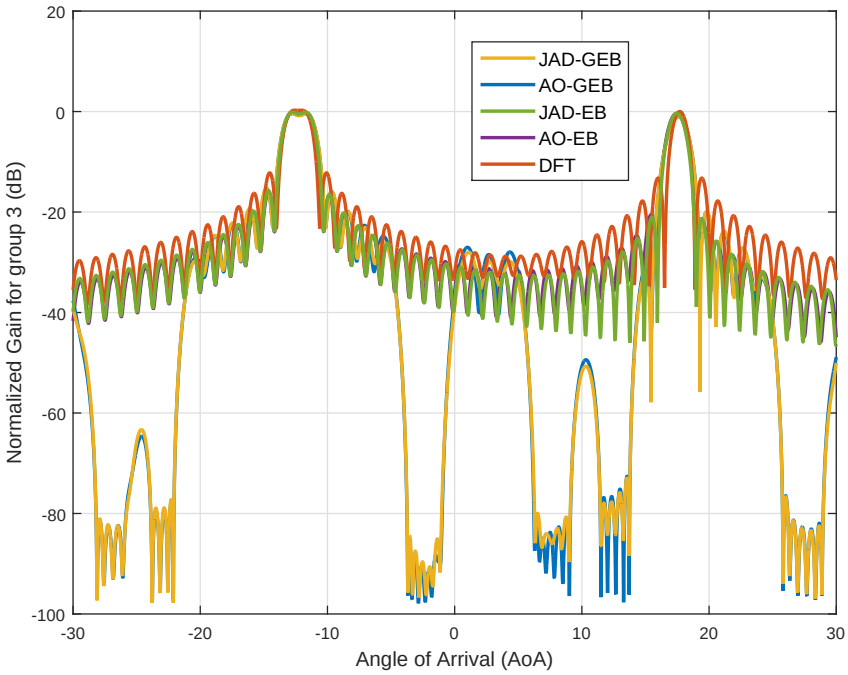

Figure 6.30: Beampatterns of all analog beamformer types in group 3 by using merge and split algorithm

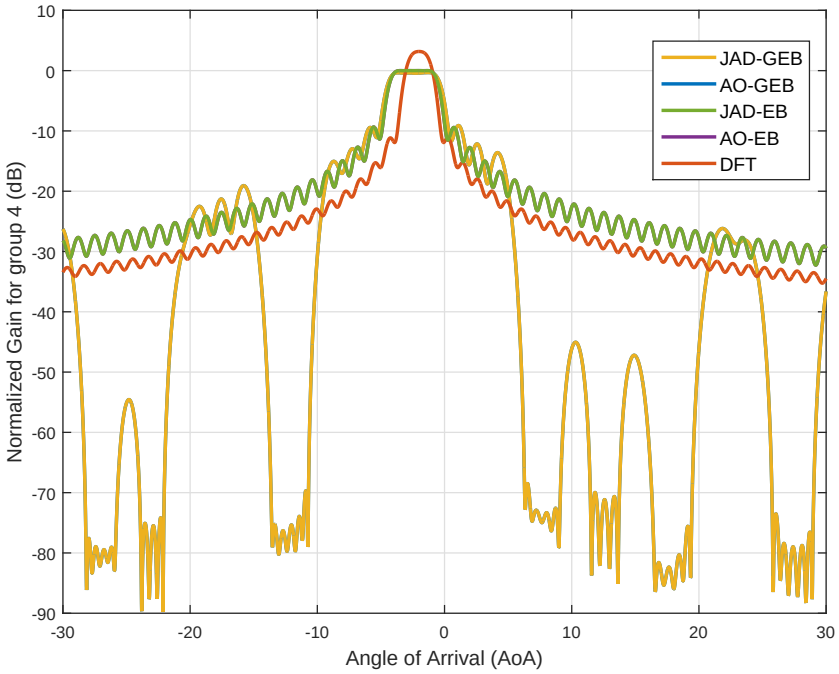

Figure 6.31: Beampatterns of all analog beamformer types in group 4 by using merge and split algorithm

6.2.6 Convergence Analysis of User Grouping Algorithms

In Chapter 5, it is said that the optimal user grouping algorithm is the merge and split algorithm with K-means initialization and novel AIR metric. This hypothesis is proven in Figure 6.32. Before the user terminals pass through the user grouping algorithm, the best user grouping is found by brute force search and it is set as the bound of the plot in Figure 6.32. The figure clearly shows that usage of merge and split algorithm together with the initialization with K-means algorithm is the best way to obtain the optimal user grouping that maximizes the performance of the hybrid structure. Using merge and split algorithm without K-means algorithm is also a solution but it converges with the brute force search bound after a long time which is not practical. Because K-means algorithm gives a reasonable user grouping input to merge and split algorithm, the speed of finding the optimal user grouping increases remarkably. K-means algorithm may find the optimal user grouping randomly. It generally finds a reasonable user grouping but not the best user grouping that maximizes AIR.

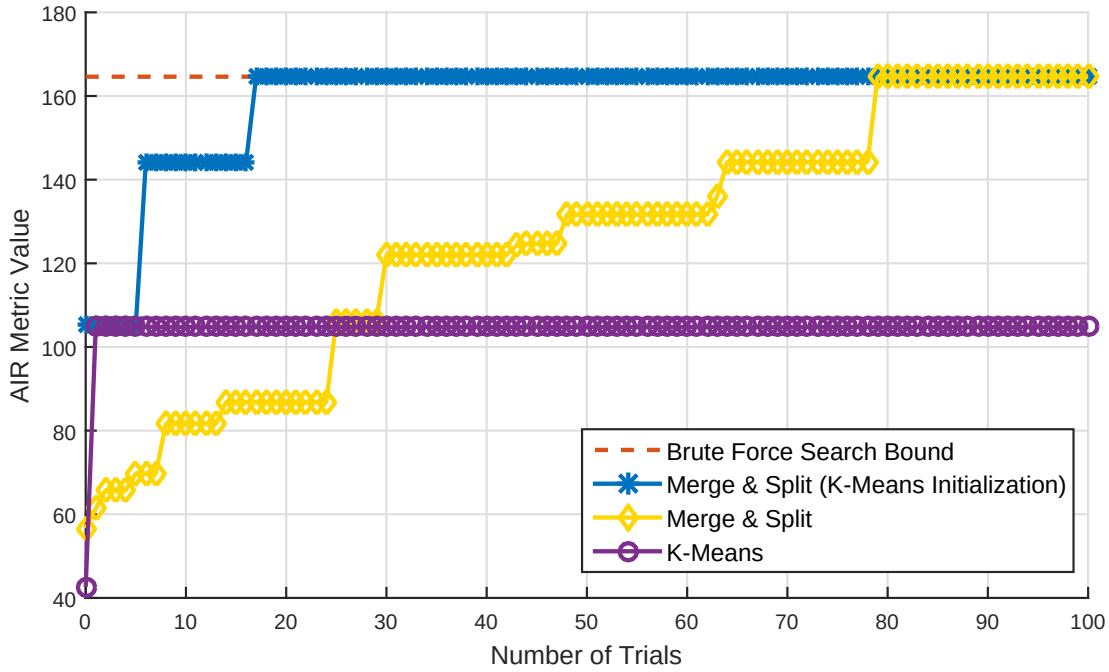

Figure 6.32: Comparison of Speed of Finding Optimal Grouping Among User Grouping Algorithm Options

CHAPTER 7

CONCLUSIONS

In this thesis, we design a novel hybrid precoding architecture for single-carrier transmission and an optimal user grouping algorithm that makes the precoder provide maximum performance.

Chapter 2 mentions about the system model, the instantaneous channel and the reduced dimensional channel. Using the reduced dimensional channel created from the instantaneous channel and the analog beamforming matrix makes the system simpler and power efficient. This chapter also includes channel covariance matrix description. The channel covariance matrices for all user terminals are used in user grouping algorithm to find a final user grouping distribution set. After that, a final group channel covariance matrices are generated and they are used in analog beamformer part to create the beams for each group.

In Chapter 3, the proposed hybrid precoding structure for downlink wideband Massive MIMO channels is expressed. The hybrid structure splits the precoder into two parts as the analog beamformer and the digital precoder. Different options are evaluated for both of these two parts. In this chapter, RF chain distribution between the groups or the multi-path components are also adverted.

Chapter 4 talks about the achievable information rate that is used as the performance parameter throughout this study. The mathematical definition of AIR, the received signal powers and possible analytical solutions to AIR are referred.

Chapter 5 includes the user grouping algorithm that tries to find an optimal user grouping distribution set that maximizes the performance of the precoder. Two options are used for the algorithm and they are evaluated according to the performance

results of their output user grouping distribution set. A novel AIR metric is proposed here for the merge and split based user grouping algorithm.

Chapter 6 shows and discusses the simulation results. It includes angle-delay plane and the scenario that is used to demonstrate the simulation results. By using different digital precoders and analog beamformers; the effect of the total transmit power on AIR, the effect of the transmit power of the other groups by keeping the desired group's transmit power unchanged on AIR of the desired group, the effect of user grouping algorithm on AIR and the effect of user grouping algorithm on the beampattern creation in analog beamformer are all observed in this chapter.

To sum up, we proposed efficient hybrid beamforming techniques for single-carrier downlink wideband massive MIMO systems. We provided a complete system analysis covering upto AIR calculation. Numerical results verify that the proposed joint angle-delay generalized eigen beamformer (JAD-GEB) is the best among other analog beamformers. As the digital precoder, CMF-SZF type precoder is the best option in order to make the system work on multi user systems. As the user grouping algorithm, merge and split based user grouping algorithm together with our novel AIR metric finds the best user grouping set for the performance of the precoder.

Power profile estimation in angle-delay domain, resolution constraints of phase shifters and amplifiers in analog beamformer stage, and making the system suitable for the mobile actively moving user terminals can be subjects of future studies.

REFERENCES

[1] J. G. Andrews, S. Buzzi, W. Choi, S. V. Hanly, A. Lozano, A. C. K. Soong, and J. C. Zhang, "What will 5G be?," *IEEE J. Sel. Areas Commun.*, vol. 32, pp. 1065-1082, Jun. 2014.

[2] E. G. Larsson, O. Edfors, F. Tufvesson, and T. L. Marzetta, "Massive MIMO for next generation wireless systems," *IEEE Commun. Mag.*, vol. 52, pp. 186-195, Feb. 2014.

[3] A. Ghosh, T. A. Thomas, M. C. Cudak, R. Ratasuk, P. Moorut, F. W. Vook, T. S. Rappaport, G. R. MacCartney, S. Sun, and S. Nie, "Millimeter-wave enhanced local area systems: A high-data-rate approach for future wireless networks," *IEEE J. Sel. Areas Commun.*, vol. 32, pp. 1152–1163, Jun. 2014.

[4] A. L. Swindlehurst, E. Ayanoglu, P. Heydari, and F. Capolino, "Millimeter-wave massive MIMO: The next wireless revolution?," *IEEE Commun. Mag.*, vol. 52, pp. 56–62, Sep. 2014.

[5] L. Lu, G. Y. Li, A. L. Swindlehurst, A. Ashikhmin, and R. Zhang, "An overview of massive MIMO: Benefits and challenges," *IEEE J. Sel. Areas Commun.*, vol. 8, pp. 742–758, Oct. 2014.

[6] J. Jose, A. Ashikhmin, T. L. Marzetta, and S. Vishwanath, "Pilot contamination and precoding in multi-cell TDD systems," *IEEE Trans. Wireless Commun.*, vol. 10, pp. 2640–2651, Aug. 2011.

[7] R. Mèndez-Rial, C. Rusu, N. González-Prelcic, A. Alkhateeb, R. W. Heath Jr., "Hybrid MIMO Architectures for Millimeter Wave Communications: Phase Shifters or Switches?," *IEEE Access*, vol. 4, pp. 247–267, 2016.

[8] A. Alkhateeb, J. Mo, N. Gonzalez-Prelcic, and R. W. Heath, "MIMO Precoding and Combining Solutions for Millimeter-Wave Systems," *IEEE Commun. Mag.*, vol. 52, no. 12, pp. 122-131, Dec. 2014.

[9] A. F. Molisch, V. V. Ratnam, S. Han, Z. Li, S. L. H. Nguyen, L. Li and K. Haneda, "Hybrid Beamforming for Massive MIMO: A Survey," *IEEE Commun. Mag.*, vol. 55, no. 9, pp. 134-141, Sept. 2017.

[10] Z. Li, S. Han, S. Sangodoyin, R. Wang and A. F. Molisch, "Joint optimization of hybrid beamforming for multi-user massive MIMO downlink," *IEEE Trans. on Wireless Commun.*, vol. 17, no. 6, pp. 3600-3614, Jun. 2018.

[11] A. Adhikary, J. Nam, J. Y. Ahn, and G. Caire, "Joint spatial division and multiplexing: The large-scale array regime," *IEEE Trans. Inf. Theory*, vol. 59, pp. 6441-6463, Oct. 2013.

[12] J. Nam, A. Adhikary, J. Y. Ahn, and G. Caire, "Joint spatial division and multiplexing: Opportunistic beamforming, user grouping and simplified downlink scheduling," *IEEE J. Sel. Topics Signal Process.*, vol. 8, pp. 876–890, Oct. 2014.

[13] D. Kim, G. Lee, and Y. Sung, "Two-stage beamformer design for massive MIMO downlink by trace quotient formulation," IEEE Trans. Commun., vol. 63, pp. 2200-2211, Jun. 2015.

[14] J. Chen and V. K. N. Lau, "Two-tier precoding for FDD multi-cell massive MIMO time-varying interference networks," *IEEE J. Sel. Areas Commun.*, vol. 32, pp. 1230–1238, Jun. 2014.

[15] O. E. Ayach, S. Rajagopal, S. Abu-Surra, Z. Pi, and R. W. Heath, "Spatially sparse precoding in millimeter wave MIMO systems," *IEEE Trans. Wireless Commun.*, vol. 13, pp. 1499–1513, Mar. 2014.

[16] A. Liu and V. Lau, "Phase only RF precoding for massive MIMO systems with limited RF chains," *IEEE Trans. Signal Process.*, vol. 62, pp. 4505–4515, Sep. 2014.

[17] S. Noh, M. D. Zoltowski, and D. J. Love, "Training sequence design for feedback assisted hybrid beamforming in massive MIMO systems," *IEEE Trans. Commun.*, vol. 64, pp. 187–200, Jan. 2016.

[18] L. You, X. Gao, A. L. Swindlehurst, and W. Zhong, "Channel acquisition for massive MIMO-OFDM with adjustable phase shift pilots," *IEEE Trans. Signal Process.*, vol. 64, pp. 1461–1476, Mar. 2016.

[19] W. U. Bajwa, A. Sayeed, and R. Nowak, "Sparse multipath channels: Modeling and estimation," *IEEE 13th Digital Signal Process. Workshop*, pp. 320–325, Jan. 2009.

[20] Z. Chen and C. Yang, "Pilot decontamination in wideband massive MIMO systems by exploiting channel sparsity," *IEEE Trans. Wireless Commun.*, vol. 15, no. 7, pp. 5087-5100, Jul. 2016.

[21] S. Haghighatshoar and G. Caire, "Enhancing the estimation of mm-wave large array channels by exploiting spatio-temporal correlation and sparse scattering," *arXiv:1602.03091*, 2016.

[22] A. Adhikary, E. A. Safadi, M. K. Samimi, R. Wang, G. Caire, T. S. Rappaport, and A. F. Molisch, "Joint spatial division and multiplexing for mm-wave channels," *IEEE J. Sel. Areas Commun.*, vol. 32, pp. 1239-1255, Jun. 2014.

[23] L. You, X. Gao, A. L. Swindlehurst, and W. Zhong, "Channel acquisition for massive MIMO-OFDM with adjustable phase shift pilots," *IEEE Trans. Signal Process.*, vol. 64, pp. 1461-1476, Mar. 2016.

[24] G. M. Guvensen and E. Ayanoglu, "A generalized framework on beamformer design and CSI acquisition for single-carrier massive MIMO systems in millimeter wave channels," *2016 IEEE Globecom Workshops (GC Wkshps)*, Washington, DC, pp. 1-7, 2016.

[25] J. Chen, and D. Gesbert, "Joint User Grouping and Beamforming for Low Complexity Massive MIMO Systems," *2016 IEEE 17th International Workshop on Signal Process. Advances in Wireless Commun. (SPAWC)*, Edinburgh, pp. 1-6, 2016.

[26] C. Rusu, R. Mèndez-Rial, N. González-Prelcic, R. W. Heath Jr., "Low Complexity Hybrid Precoding Strategies for Millimeter Wave Communication Systems," *IEEE Trans. Wireless Commun.*, vol. 15, no. 12, pp. 8380-8393, Dec. 2016.

[27] W. Saad, Z. Han, M. Debbah, and A. Hjorungnes, "A distributed coalition formation framework for fair user cooperation in wireless networks," *IEEE Trans. Wireless Commun.*, vol. 8, no. 9, pp. 4580-4593, Sept. 2009.

[28] W. Saad, Z. Han, T. Basar, M. Debbah, and A. Hjorungnes, "Coalition formation games for collaborative spectrum sensing," *IEEE Trans. Veh. Tech.*, vol. 60, no. 1, pp. 276-297, Jan. 2011.

[29] N. Beigiparast, G. M. Guvensen, and E. Ayanoglu, "The Effect of Spatial Correlation on the Performance of Uplink and Downlink Single-Carrier Massive MIMO Systems," *arXiv:1906.07766*, 2019.

[30] R. Mendez-Rial, C. Rusu, N. Gonzalez-Prelcic, A. Alkhateeb, and R. W. Heath, "Hybrid MIMO Architectures for Millimeter Wave Communications: Phase Shifters or Switches?," *IEEE Access*, vol. 4, pp. 247-267, 2016.

[31] A. Adhikary, E. Al Safadi, M. K. Samimi, R. Wang, G. Caire, T. S. Rappaport, and A. F. Molisch, "Joint Spatial Division and Multiplexing for mm-Wave Channels," *IEEE J. Sel. Areas Commun.*, vol. 32, no. 6, pp. 1239-1255, June 2014.

[32] H. Xie, F. Gao, S. Zhang, and S. Jin, "A Unified Transmission Strategy for TDD/FDD Massive MIMO Systems With Spatial Basis Expansion Model," *IEEE Trans. Veh. Tech.*, vol. 66, no. 4, pp. 3170-3184, April 2017.

[33] A. Pitarokoilis, S. K. Mohammed and E. G. Larsson, "On the Optimality of Single-Carrier Transmission in Large-Scale Antenna Systems," *IEEE Wireless Commun. Letters*, vol. 1, no. 4, pp. 276-279, August 2012.